

RESEARCH

Open Access



An analytical survey of zinc white historical and modern artists' materials

Nicoletta Palladino^{1,2}, Mathilde Occelli³, Gilles Wallez^{1,3,4}, Yvan Coquinot¹, Quentin Lemasson^{1,5}, Laurent Pichon^{1,5}, Slavica Stankic⁶, Victor Etgens¹ and Johanna Salvant^{1,4*}

Abstract

This study is the first systematic survey of a large corpus of zinc white (ZnO) artists' materials. Zinc white is a white pigment developed within the wave of 19th-century technological developments in the paint industry. The composition, particle morphology and size, and luminescence of 49 zinc white samples from artists' materials were characterized, including three references of known synthesis methods (indirect and direct) and synthesized by the authors (ZnO nanosmoke). The corpus included historical and modern zinc white pigment powders and paint materials from the leading European and American color manufacturers. The study aims to characterize and evaluate the variability of the properties of zinc white and its paint formulations. The reference materials presented properties in agreement with the literature: indirect ZnO exhibited submicron prismoidal blue-luminescent particles of higher purity than direct ZnO , which had larger acicular green-luminescent particles. ZnO nanosmoke presented acicular (tetrapod-like) blue/green-luminescent nanoparticles. Composition, particle morphology, size, and documentary sources suggested a production via the indirect method for the analyzed corpus. However, the luminescence behavior was more complex to interpret. The fundamental emission of ZnO was not always detected, even in pure ZnO powders. Three trends were identified: smaller ZnO particles for the most recent samples; green luminescence connected to larger particle size; fewer trace elements, and of the same type (i.e., lead, sulfur) for historical materials. Another interesting finding was the detection of hydrozincite in some powders, likely a degradation product of ZnO . In terms of methodology, cathodoluminescence proved a valuable tool for pigment identification. The study provides a database of zinc white references for pigment and artwork analysis.

Keywords Zinc white, Artists' materials, Painting, SEM–EDX, PIXE, XRD, Cathodoluminescence

*Correspondence:

Johanna Salvant

johanna.salvant@culture.gouv.fr

¹ Centre de Recherche et Restauration des Musées de France (C2RMF), Palais du Louvre, Porte Des Lions, 14 Quai François Mitterrand, 75001 Paris, France

² Laboratoire Institut Photonique d'analyse Non-Destructive Européen Des Matériaux Anciens (IPANEMA), Site du Synchrotron SOLEIL, Université Paris-Saclay, Saint-Aubin, BP48, 91192 Gif-Sur-Yvette, France

³ UFR 926, Chimie, Sorbonne Université, 4 Place Jussieu, 75252 Paris cedex 05, France

⁴ Institut de Recherche de Chimie Paris (IRCP), UMR 8247, Chimie ParisTech, PSL University, CNRS, 11 Rue Pierre Et Marie Curie, 75005 Paris, France

⁵ Fédération de Recherche NewAGLAE, FR3506 CNRS/Ministère de La Culture/Chimie ParisTech, Palais du Louvre, 75001 Paris, France

⁶ UMR 7588, Sorbonne Université, CNRS, Institut des NanoSciences de

Paris INSP, 4 Place Jussieu, 75252 Paris cedex 05, France



Introduction

Zinc white (zinc oxide, ZnO) is a modern pigment, a product of the technological and industrial development of the 19th century. Though known since antiquity for ointments and as a sub-product in brass manufacturing, it was only at the end of the 18th century that it started to be studied as an alternative to the white par excellence, the toxic lead white [1]. At the time, zinc white was praised for not being a risk to human health, not darkening upon exposure to sulfurous gases, and for being permanent. Its covering power in oil is weaker than lead white's [2], which makes it more suitable for transparency effects and to be mixed with other pigments [3].

ZnO is used not only for paint materials (e.g., watercolors, oil colors, pastels, house paint, mastics, acrylics) but also as a vulcanization accelerator for rubber production, as well as for applications in ceramics, electronics, polymers, cosmetics, pharma [4] and nanotechnology [5–8]. As a pigment, it has been used as white *as-is* (in house paint and fine arts), but also for ground layers (e.g., by Pre-Raphaelites [9] and some 20th-century American artists [10, 11]). Still commercialized today, zinc white has been widely replaced by titanium white since the second half of the 20th century and can often be found in titanium white tubes to adjust its tinting strength [12].

The pigment is known under different names, such as *Chinese white* (for watercolors), *snow white/Schneeweiss/blanc de neige, blanc de trémie, blanc léger, Constant white, Hubbooks white, permanent white* [1, 13].

It is manufactured by two main methods, both pyrometallurgical [1]:

- The French or indirect method, ~80% of today's ZnO production [9], which uses metallic zinc as a raw material;
- The American or direct method, where zinc ores and a reducing agent (e.g., carbon coke) are heated up to reduce zinc compounds to zinc before oxidation.

Other methods, such as the wet chemical process, are used to produce ZnO for different applications, such as in the textile [4] and rubber industries.

The first successful trials of the synthesis of zinc white were performed by the chemists Jean-Baptiste Courtois (1777–1838) and Louis-Bernard Guyton de Morveau (1737–1816) in Dijon (France) around 1780 after some early tests in Germany [14]. In 1796, the English color-maker John Atkinson of Harrington issued a patent for the manufacturing of ZnO in the United Kingdom [14]. In 1834, Winsor & Newton first sold *Chinese white* for watercolors [15]. Large-scale production of the pigment for oil colors only started in the second half of the 19th century, when the architectural painter Edme-Jean

Leclaire (1801–1872), influenced by the experiments of the French inventor Stanislas Sorel (1803–1871) [16], developed the so-called French or indirect method. He also discovered a manganese-based drier able to overcome the longer drying time of the pigment, the major drawback to its use [14].

Shortly after developing the indirect process, Leclaire collaborated with the leading European zinc manufacturer, the Belgian company *Vieille Montagne*, which exploited calamine deposits,¹ mainly in Belgium [17]. The produced pigments were then sold to the main color merchants of the time, such as *Lefranc* [18], *Sennelier*², and *Winsor & Newton* [15].

From the second half of the 19th century, many technological developments improved pigment manufacturing (e.g., reverberatory³ and muffle/retort⁴ furnaces). However, parameters such as temperature and airflow were still hard to control [19].

In the 1850s, the *New Jersey Zinc Company*, taking advantage of the discovery of franklinite⁵ deposits, patented an alternative method of ZnO manufacturing in the United States, the so-called American or direct method. In 1892, the French process also started being used in the United States, becoming the most widespread production method of ZnO worldwide [1].

At the beginning of the 20th century, scientists realized that zinc white was linked to some degradation issues like chalking of house paint [20, 21] and metal soaps [22–26]. These phenomena can change the visual appearance of paintings and provoke cracking, delamination, and paint loss in the most severe cases [10, 23, 24, 26, 27]. Thus, it would be important for conservators to have an easy method to identify zinc white in artworks and pinpoint early warning signals of its degradation [19].

A considerable amount of studies have already been performed on the interaction of zinc white with oils and the formation of metal soaps [3, 28–35], its photoluminescence [20, 36–40], composition [18], rheological [41] and mechanical properties [42], as well as its use and degradation in watercolors [9], oil paint [27, 43, 44] and grounds [10, 11]. Moreover, the pigment has been used for restoration since the 19th century [45]. It is still on the market today, even though many artists are unaware of its properties, use, and related degradation phenomena [24].

¹ Smithsonite, a zinc carbonate mineral containing some lead.

² Personal communication.

³ Raw materials are isolated from the fuel, but not the combustion gas.

⁴ Heat is applied to a vessel that contains the raw materials, so that emitted gas and products are carried away to a separation/collection section.

⁵ A mineral composed of iron, zinc, and manganese oxides.

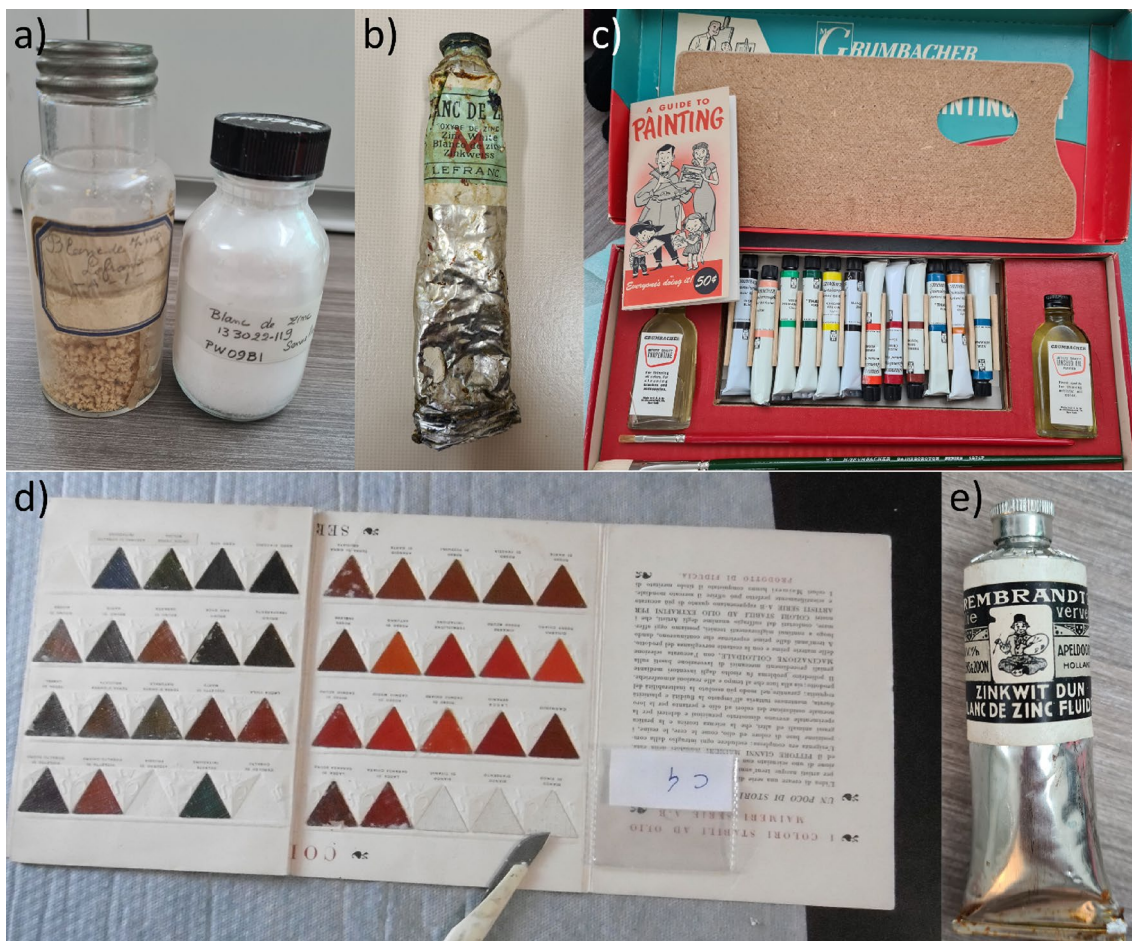


Fig. 1 Examples of historical zinc white samples belonging to the corpus of study: **a** Lefranc and Sennelier powders, C2RMF material collection; **b** Lefranc paint tube, 1930s, private collection of Nathalie Balcar (C2RMF); **c** Grumbacher color set, 1950s, private collection of Gilles Bastian (C2RMF); **d** Maimeri color chart, 1940s © Sandro Baroni, Fondazione Maimeri; **e** Talens paint tube, 1930s, private collection of Gilles Bastian (C2RMF)

Different types of zinc white have been identified, but as Eastaugh et al. [19] pointed out, the cause-and-effect relations of these remarks are still not completely understood. They tackled this issue by studying documentary sources and establishing historical synthesis patterns. Other research groups analyzed historical zinc white artists' materials, focusing on specific examples, such as the French brands *Lefranc* and *Ripolin* [18, 38, 46–48].

Our study is the first systematic survey of a large and unique corpus of zinc white historical and modern artists' materials (e.g., pigment powders, paint tubes) from Europe and the United States of America, gathered with the help of museums, cultural institutions, and research centers. This research aims to correlate the synthesis method of zinc white to its properties to identify potential markers for identifying and classifying the pigment and create a reference database for painting conservation and authentication.

The corpus of samples and the methodology used are presented first. The results are then described and discussed in light of historical and modern scientific literature.

Materials and methods

Samples

The corpus consisted of 49 samples referred to as zinc white donated by museums, researchers, foundations, a company, or synthesized (some examples in Fig. 1). It covered a significant timeframe, from the end of the 19th century until today, even though it was impossible to date all the samples accurately. In this paper, the samples dating back to the 19th–20th century are indicated as “historical”; those produced or bought in the 21st century are referred to as “modern”.

Table 1 below provides an overview of the samples, classified into three categories:

Table 1 Summary of the samples in the corpus of analysis

Brand	Samples
Reference samples	
<i>Synthesized ZnO</i>	ZnO nanosmoke synthesized as in Zhang et al. [49]
ZnO manufacturers	
<i>KF chemicals</i> Japan, since 1951	Two powders (2020, indirect and direct method)
<i>Kremer</i> Germany, since 1977	One powder (historical)
<i>Maastrichtsche zinkwit Maatschappij</i> The Netherlands, 1870–1989, then acquired by the <i>Vieille Montagne</i>	Two powders (2010 and 2021)
<i>Merck</i> Germany, since 1668	Four powders of different grades (1907–1989)
<i>Sikkens</i> The Netherlands, since 1792	One powder (historical)
<i>Vieille Montagne</i> Belgium, 1837–1989, then <i>Union Minière</i> , today <i>Umicore</i>	One powder (historical)
Color manufacturers	
<i>Blockx</i> Belgium, since 1865	Six powders of different grades (1847–1989)
<i>Bocour</i> US, since 1932	Two paint tubes (1976 and 2021)
<i>Charvin</i> France, since 1830	One titan-zinc white paint tube (2021)
<i>Craftint manufacturing company</i> US, 1929–2018	One paint tube (1933–1975)
<i>Fezandie & Sperrle</i> US, until 1979	One titan-zinc white paint jar (1940–1975)
<i>Grumbacher</i> US, since 1905; today, in <i>Chartpark, Inc</i>	One paint tube (2010)
<i>Lefranc</i> France, 1720–1964, then <i>Lefranc & Bourgeois</i>	One paint tube (1950s)
<i>Lefranc & Bourgeois</i> France, since 1964	One powder (historical)
<i>Maimeri</i> Italy, since 1923; in <i>Fila</i> group since 2014	Three paint tubes (1950s and two tubes dating back to 1960–1975)
<i>Michael harding</i> US, since 1982	One paint tube (1930s)
<i>Old holland</i> The Netherlands, since 1664	One paint sample (1950)
<i>Permanent pigments</i> US, 1933–1955	One powder with a binder (before 1964)
<i>Ripolin</i> France, since 1888	Two paint tubes (after 1964, 2021)
<i>Sennelier</i> France, since 1887	One pastel (after 1964)
<i>Talens</i> The Netherlands, 1889–1969, then <i>Sikkens</i> group, then <i>Akzo Nobel</i>	One paint sample from a color chart (1939–1946)
<i>Vilhelm Pacht</i> Denmark, since 1887	One paint tube (1970s)
Brands are listed in alphabetical order. The date of production of the samples is indicated between brackets in the column on the right when available	

- Reference materials of known production methods;
- Samples from ZnO manufacturers;
- Samples from colormen and paint manufacturers.

The samples were either in the form of powder (referred to as “powder”) or of powder ground in a binder (referred to as “paint”). Details about the analyzed

samples classified by manufacturer/supplier, including their product description, are available in Additional file 1: Table S1.

Reference materials

Three modern materials, all in the form of powder and of known production methods, were used as a reference for the study:

- ZnO nanosmoke synthesized by the authors as described in Zhang et al. [49], well-known in terms of size, shape, crystallographic characteristics, optical properties, point defects, and surface reactivity;
- ZnO manufactured by the German chemical company Brüggemann,⁶ either by direct or indirect method.

Paint mockups were also prepared by grinding these powders in linseed oil.

Samples from ZnO manufacturers

The fifteen samples from ZnO manufacturers were all powders without specifications of their production method. Two of them were modern materials produced by Kremer; the remaining thirteen were historical samples, including different grades (*cachets or, argent, blanc, rouge, bleu*,⁷ in order of purity) from the Société de la Vieille Montagne (Liège, Belgium). Two of them (*cachets argent, bleu*) were described by the manufacturer as "lab samples", while the other four (two *cachet blanc*, one *cachet or*, and one *cachet rouge*) were from the production facility Valentin-Cocq (Liège, Belgium). In addition, samples of four different grades (Serena witzegel, *Grijsegel n°3*, Serena roedzegel, *Serena roedzegel n°1*⁸) from another historical ZnO manufacturer in the Netherlands, the *Maastrichtsche zinkwit Maatschappij*, were also investigated.

Samples from colormen and paint manufacturers

The remaining thirty-one samples of the corpus were materials labeled as zinc white from a large variety of colormen (~70% historical, from the end of the 19th century until the 1970s, ~30% modern). Many of the leading 19th–20th century European and American ZnO manufacturers and colormen (e.g., Lefranc, Sennelier, Ripolin, Winsor & Newton, Maimeri, Grumbacher) were represented (Table 1). Products from these color-makers were used by the foremost 19th- and 20th-century artists,

whose artworks are now in different conservation states [11, 22, 23, 50–55]. Paint materials were mainly paint tubes except for a few samples: two fragments from *Maimeri* and *Ripolin* color charts, a sample of 1950s *Lefranc* paint from a canvas, and a *Lefranc & Bourgeois* pastel.

Methods

The corpus was analyzed by multiple techniques to shed light on different properties of zinc white:

- Composition, using Scanning Electron Microscopy-Energy Dispersive X-ray spectroscopy (SEM-EDX), Particle-Induced X-ray Emission spectroscopy (PIXE), X-Ray Diffraction (XRD);
- Particle morphology and size using optical microscopy (OM), SEM, and High angular Resolution XRD (HR-XRD);
- Luminescence signature using OM under UV light, cathodoluminescence (CL), and Ion Beam-Induced Luminescence (IBIL);
- Binders, using Fourier-Transform InfraRed spectroscopy (FTIR).

Table 2 summarizes the techniques used with the addressed property, sample preparation, and number of analyzed samples.

Optical microscopy

Each sample was observed *as-is*, in the form of powder or mixed with a binder, with no sample preparation. A small amount was put on a microscope glass slide and observed with a Nikon Eclipse LV100ND optical microscope using a Nikon Xenon Power Supply XPS-100 Xenon lamp and a Nikon DS-Ri1 camera. Three observation methods were applied: dark-field mode, fluorescence mode under ultraviolet (UV, 330–390 nm), and blue light (450–490 nm).

The NiSS-Element software was used to acquire the images.

Scanning electron microscopy-energy dispersive x-ray spectroscopy

Two protocols were used for imaging zinc white powders or paint materials.

The size of ZnO particles was estimated by measuring about ten particles for each sample in ImageJ.

ZnO powders

The samples, previously observed using OM, were dispersed in isopropanol with the help of an ultrasonic device. A drop of the dispersion was applied on a piece of Si (100) attached to the sample holder by carbon tape. The samples were then left to dry under a fume hood.

⁶ L. Brüggemann GmbH & Co. KG, Salzstraße 131, 74076 Heilbronn, Deutschland, <https://www.brueggemann.com/>.

⁷ Golden, silver, white, red, blue seals.

⁸ White, grey, and red seals.

Table 2 Summary of the techniques used to characterize the corpus of samples

Technique	Addressed property	Sample preparation		Studied samples ^a	
		Powder	Paint	Powder	Paint
OM under visible and UV light	Color, photoluminescence	As-is	As-is	All	All
SEM-EDX	Particle morphology and size, elemental composition	Dispersed in ethanol and dried on a Si wafer	Cross-section	20	10
PIXE	Elemental composition, trace elements	Between polypropylene sheets		19	22
XRD	Crystalline structure, composition, particle size ^b	As-is for micro-XRD; in borosilicate capillaries for HR-XRD		22	23
CL	Cathodoluminescence	Mixed with araldite and spread on a roughened glass slide	Cross-section	19	15
FTIR	Type of binder, presence of metal soaps, and other compounds	As-is	As-is	12	18

^a Detailed in Additional file 2: Table S2.0

^b High-angular Resolution X-Ray Diffraction at the ESRF

The methodology was developed on reference powder samples (i.e., Brüggemann ZnO, indirect and direct) using a FEG SUPRA 40 ZEISS at the *Institut des Nano-Sciences de Paris* (INSP; Paris, France); the other powder samples were observed using a FEG Supra55VP ZEISS at the IPANEMA laboratory (Gif-sur-Yvette, France).

The InLens detector (secondary electrons) acquired the images at an operating voltage of 5 kV and a 3–4 mm working distance.

Zinc white samples with binder

Samples containing a binder were embedded in araldite, as explained below for cathodoluminescence. The cross-sections were polished up to 1 µm and sputter-coated with 0.7 nm of platinum for analysis with a Jeol JFC-2300HR fine coater. Images and analyses were conducted using a JEOL 7800F with two SDD Bruker AXS 6|30 detectors at the *Centre de Recherche et Restauration des Musées de France* (C2RMF; Paris, France). The images were acquired using secondary (SE) and backscattered electrons (BSE) at an operating voltage of 5 kV and a working distance of 6 mm.

EDX analyses were performed at an operating voltage of 15 kV and an optimal working distance of 9.5 mm. 6–12 points were selected based on the BSE images obtained at $\times 10\,000$ magnification. The software Esprit (Bruker, version 2.3) acquired and stored data.

Particle-induced X-ray emission spectroscopy and Ion Beam-Induced Luminescence

The samples were mounted between two polypropylene sheets (FLUXANA) of 6 µm thickness at a 2–3 mm distance to the extracted beam.

The analyses were performed at the *Accélérateur Grand Louvre d'Analyses Élémentaires* (NewAGLAE, ANR-10-EQPX-22) [54]. Four Peltier-cooled SDD detectors were used: one for low energies with a helium flux (1–10 keV), placed at 50° relative to the beam axis, three for high energies, at a relative angle of 45° (1 with a 200 µm Al filter, 2 with 25 µm Co filter) [49]. Two areas of $1000 \times 1000 \mu\text{m}^2$ with a pixel size of $50 \times 50 \mu\text{m}^2$ were measured for each sample, with a 100,000 total dose (corresponding to a charge of 0.8 µC) using a 3 MeV proton beam.

The used standards were DRN for calibrating the low-energy detector and two copper-based standards, BS938 and CTIF6, for the high-energy detectors.

Sample luminescence was collected by a 1 mm diameter optical fiber placed at 45° to the beam axis, conducted to a research grade OCEAN OPTICS QE65000 spectrometer. It was measured in the wavelength range 200–1000 nm, with a resolution of 3 nm FWHM (100 µm entrance slit) [56].

X-Ray diffraction

Micro-XRD No specific sample preparation was required; ZnO powders or paint fragments were put *as-is* on the sample holder.

The experimental setup consisted of a XENOCS GENIX 3D copper source with a high-brilliance X-ray tube (power of 30 W, diameter of 30 µm) and Xenocs FOX 3D optics, which delivers a beam at the length of 1.5418 Å (Cu Kα1-2), at 50 kV, 600 µA, with a pixel size resolution of 200 µm. The diffraction patterns were acquired by a Rigaku R AXIS IV+ + imaging plate detector developed by Bede Scientific Instruments Limited.

The analyses were carried out at an angle of incidence of about 10°.

The acquired 2D data was transformed into a diffractogram by the FIT2D software; crystalline phases were identified by the software QualX 2.0 [57].

High angular resolution-X-Ray diffraction A selection of samples was analyzed at the ID22 beamline at the European Synchrotron Radiation Facility (ESRF) [58–61]. Analyses were performed on samples in borosilicate capillaries ($\phi=0.5$ mm, WJM-Glas/Müller GmbH); a LaB₆ standard was used as a reference for instrumental resolution.

Measurements were performed at $\lambda=0.3542$ Å (35 keV), thanks to the new Extremely Brilliant Source with a highly monochromatic beam of about 1×1 mm² and low divergence. Diffracted photons were measured by scanning the 2θ circle over the 0–43° range holding an EIGER2 2 M-W CdTe pixel detector positioned behind thirteen Si (111) analyzer crystals.

A preliminary identification of the present phases was performed using the software QualX mentioned above. A Williamson-Hall analysis was performed by fitting the diffraction peaks through the software WinPLOTR [62] of the FullProf Suite to calculate the average size of the ZnO crystallite in and perpendicular to the (001) plane, the aspect ratio, and the lattice strain of the crystallites, by taking into account the broadening of the diffraction peaks. Details about the procedures are available in the Additional file 1.

Cathodoluminescence

All the samples were embedded in araldite 2020 transparent liquid adhesive epoxy (volume ratio epoxy adhesive/catalyzer of 10:3) to avoid any luminescence from the resin, according to the following protocols:

- For ZnO powders, a small amount of sample was mixed with the araldite and applied on a roughened microscope glass slide. The resulting slides were lightly polished with a 1200 grit SiC disc by Buehler (15 µm) to obtain a flat surface;
- For zinc white samples containing a binder, small paint flakes were embedded in araldite. The molded samples were sliced to obtain two cross-sections and then polished.

Experimental conditions were fixed at an operating voltage of 11 kV and a current of ~390 µA.

The cathodoluminescence system Cambridge Imaging Technology Ltd CL8200 Mk5-1, consisting of a controlled electronics unit and a vacuum chamber associated with an electron gun, was used to study

the cathodoluminescence of the samples. Images were acquired with an Olympus BH-2 optical microscope (10× objective). The exposure conditions were fixed at 3 s with a gain of 5.1x, slightly adjusted for some samples to avoid overexposed images. A Nikon DS-Ri2 camera and the NiSS-Element software were used to acquire and store the images.

An Ocean Optics QE65000 spectrometer acquired luminescence spectra; four accumulated spectra were recorded by the Ocean Optics SpectraSuite software with an exposure of 2 s. The two main luminescence peaks' position, intensity, and width were noted.

Fourier-transform infraRed spectroscopy

No sample preparation was required; a small amount of material was directly placed on the accessory before each measurement.

Samples were analyzed using an FT-IR Frontier PerkinElmer Spectrometer with an MCT detector. An ATR Goldengate accessory from Specac with a diamond tip or a diamond anvil cell from High-Pressure Diamond Optics, Inc. was used for the measurements, depending on the sample amount available. Spectra were collected in the 4000–400 cm⁻¹ range with a resolution of 4 cm⁻¹ and an accumulation of twenty (ATR Goldengate accessory) or forty (diamond anvil cell) spectra.

Data were acquired and processed using the software Spectrum (PerkinElmer).

Results

This section consists of three parts: results about the composition of the samples are presented first, followed by insights on morphology and size of ZnO particles, and, finally, luminescence properties. An overview of the findings for each sample is provided in Table 3; detailed results per analytical technique are available in Additional file 2: Table S2.

Composition

After a short presentation of the results on the binders, the identified inorganic phases composing the samples are described: the purity and formulations of the ZnO materials are shown first, with major and minor compounds found, followed by the detected trace elements.

Binders⁹

FTIR analyses confirmed that all the analyzed paint samples contain oil-based binders except for the *Permanent Pigments* watercolor tube, made of gum arabic. The *Lefranc & Bourgeois* pastel had an oil binder. The *Lefranc* powder contained some wax.

⁹ Zinc carboxylates were found in all the analyzed paint materials.

Table 3 Synthesis of the analytical results obtained on the studied samples

Sample	Date	wt% ZnO ¹¹	Other main compounds ¹²	Trace elements ¹³	Morpho -logy ¹⁴	Size ¹⁵ (nm)	Luminescence under UV	Cathodoluminescence
Reference samples								
Brüggemann direct	2020	99.7	-	S, Cl, Ca, Fe	Mostly acicular	Large 	Green	Green
Brüggemann indirect	2020	100.0	-	Fe, Ni	Prisms	Small 	Some green grains	Blue
ZnO nanosmoke	2021	99.9	-	Fe	Acicular	Small 	Green with few green grains	Blue
ZnO manufacturers								
KF Chemicals	-	95.1	Hydrozincite	Pb, Fe, Ni	Prisms	Small 	Green	Green
Kremer 2010	2010	94.7	Hydrozincite	Ni, Fe	Prisms	Small 	Green with green and blue grains	Blue
Kremer 2021	2021	99.8	-	Ca, Cl, Fe	Prisms	Small	Green with blue grains	Blue
Maastrichtsche zinkwit Grijzegel n°3	1907-1989	Y	Hydrozincite	N/A	N/A	N/A	Orange	Light green
Maastrichtsche zinkwit Serena roedzegel	1907-1989	93.8	Hydrozincite	S, Pb, Fe, Ni	Prisms	Small 	Green	N/A

Table 3 (continued)

<i>Maastrichtsche zinkwit Serena roedzegel n°1</i>	1907-1989	Y	Hydrozincite	N/A	Prisms	Large	Orange	Light green with blue grains
<i>Maastrichtsche zinkwit Serena witzegel</i>	1907-1989	Y	Hydrozincite	N/A	Prisms	Small	Orange	Blue with green grains
<i>Merck</i>	-	92.5	Hydrozincite	Ni	Prisms, acicular	Large 	Green with green grains	Blue-green
<i>VM¹⁶ cachet argent, lab</i>	1847-1989	99.9	-	Pb, Fe	Prisms	N/A	Green with green and blue grains	Blue-green
<i>VM¹⁶ cachet bleu, lab</i>	1847-1989	99.7	-	Pb, S, Fe	Prisms	Medium 	Green with green grains	Green
<i>VM¹⁶ cachet blanc, MNF190</i>	1847-1989	99.0	Hydrozincite	-	Prisms, acicular	Large 	Green with green and blue grains	Blue-green
<i>VM¹⁶ cachet blanc, MNF193</i>	1847-1989	99.8	-	Pb, S, Fe	Prisms, acicular	Large	Green	Green
<i>VM¹⁶ cachet or</i>	1847-1989	98.9	Hydrozincite	Pb, S, Fe, Ni	Acicular, prisms	Large 	Green with green and blue grains	Green
<i>VM¹⁶ cachet rouge</i>	1847-1989	99.1	Hydrozincite	Pb, S, Fe	Prisms, acicular	Large 	Green with green grains	Green
Color manufacturers								
<i>Blockx paint tube</i>	2021	99.8	-	Pb, Fe, Ti, Ni	N/A	N/A	Green	N/A
<i>Blockx, titan-zinc white paint tube</i>	2021	68.4	TiO ₂	Al, Si, Pb, Cl, Fe, Ca	N/A	N/A	Blue	N/A

Table 3 (continued)

<i>Bocour</i> paint tube	1933-1975	73.9	BaSO_4	Sr, Ni	N/A	N/A	Green and blue with green grains	Blue with green grains
<i>Charvin</i> paint tube	2010	63.6	CaCO_3	Si, Ti, Mg, Fe, Zr	N/A		Blue with blue and green grains	N/A
<i>Craftint Manufacturing Company</i> paint tube	1950s	99.5	-	Ti, Al, S, Fe, Cl, Ni	Prisms	Small	Green with a few green and blue grains	Light blue
<i>Fezandie & Sperrle</i>	1850 - 1979	99.6	-	Pb, S, Cd, Ni	Prisms	Medium 	Green with green grains	Green
<i>Grumbacher</i> pre-tested paint tube	1950s	99.5	-	Pb, Ni, Al	N/A	N/A	Green with green and blue grains	Blue with green and blue grains
<i>Grumbacher Gainsborough</i> paint tube	1960 - 1975	99.8	-	Al, Ti, Ni	N/A	N/A	Green	Blue with green grains
<i>Grumbacher</i> pre-tested, paint tube	1960 - 1975	99.4	-	Si, Al, Ca, Fe, Ni	N/A	N/A	Green	Blue with green grains
<i>Lefranc</i> paint tube	1930s	99.4	-	Pb, Al, S, Fe, Ca, Ni	N/A		Green and blue with green grains	Green
<i>Lefranc</i> paint sample	1950	Y	-	N/A	N/A		Light green	N/A
<i>Lefranc</i> powder with binder	1850 - 1964	90.5	SiO_2	Ca, Fe	N/A		Green with green grains	N/A
<i>Lefranc & Bourgeois</i> paint tube	after 1964	99.4	-	Ti, Al, Ca, Fe, Cl	Prisms	Medium 	Blue with green and blue grains	Blue
<i>Lefranc &</i>	2021	99.8	-	Cl, Fe, Ni	Prisms	Small	Green with	Blue with

Table 3 (continued)

<i>Bourgeois</i> modern paint tube							green and blue grains	green grains
<i>Lefranc &</i> <i>Bourgeois</i> pastel	after 1964	99.3	-	Pb, S, Cl, Ni, Fe	N/A	Medium 17 	Green with a few green grains	N/A
<i>Maimeri</i> color chart	1939 - 1946	60.4	BaSO ₄ , CaCO ₃ , ZnS	Sr, Ni, Fe	N/A		Green with green grains	N/A
<i>Maimeri</i> paint tube	1970s	59.2	BaSO ₄ , CaCO ₃ , ZnS	Sr, Fe, Ni	Prisms	Small 	Green	Light blue
<i>Michael</i> <i>Harding</i> paint tube	2021	99.8	-	Fe, Ni	N/A	N/A 	Green with blue grains	N/A
<i>Old Holland</i> paint tube	2010	94.0	TiO ₂	Si, Al, Fe, Ni	N/A		Blue	N/A
<i>Permanent</i> <i>Pigments</i> watercolor paint tube	1933 - 1955	95.2	Pb	K, Ca, Si, Fe, Ni	N/A	N/A 	Green with green, blue grains	Blue with green grains
<i>Ripolin</i> color chart	1900	Y	-	N/A	Prisms, acicular	Large 	Green with green grains	Green with green grains
<i>Sennelier</i>	after 1887	99.9	-	Fe, Ni	Prisms	Small 	Green with a few blue grains	Green
<i>Sennelier</i>	2021	99.9	-	S, Fe, Ni	Prisms	Small 	Green with blue grains	N/A
<i>Sennelier</i> paint tube	after 1920s	60.0	Ba, TiO ₂ , SiO ₂	Al, Ca, Zr	N/A	N/A 	Green with blue and green grains	N/A

Table 3 (continued)

<i>Sennelier</i> acrylics paint tube	2021	Y	BaSO ₄	N/A	N/A	N/A	Green with blue and green grains	N/A
<i>Talens</i> paint tube	1930s	99.8	-	S, Pb, Ca, Ni	Acicular, prisms	Large 	Green with green grains	Light blue
<i>Talens</i> paint tube (dried)	1930s	99.8	-	S, Pb, Fe	N/A		Green and blue with green grains	Light blue
<i>Vilhelm Pacht</i> paint tube	1890 - 1909	98.2	-	Si, Al, Cl, Sn, Fe, S, Ca, K, Pb, Zr, Ni	Prisms	Small 	Green and blue with green grains	Light blue
Samples of different compositions than zinc white								
<i>Blockx</i> paint tube	1976	1.1	Pb (91.3 wt%), Sn, Cl	N/A	N/A	N/A	N/A	N/A
<i>Bocour</i> titan- zinc white paint jar	1940- 1975	3.3	SiO ₂ (38.1 wt%), CaCO ₃ , TiO ₂ , BaSO ₄ , ZnS, K	N/A	N/A	N/A	N/A	N/A
<i>Permanent Pigments</i>	1933 - 1955	0.0	TiO ₂ (99.9 wt%)	N/A	N/A	N/A	N/A	N/A
<i>Sikkens</i>	-	Y?	Hydrozincite ¹⁸ , Pb	N/A	N/A	N/A	Orange	Blue with a few green grains

White background for samples in the form of powder, gray for samples in the form of paint. N/A indicates that the analysis was not performed

^a From PIXE and XRD. When no PIXE was available an "Y" indicated the presence of ZnO

^b 1-10 wt%, listed in decreasing order; from PIXE and XRD

^c <1 wt%, listed in decreasing order; from PIXE

^d From SEM

^e Classification from SEM data (small if both diameter and lengths < 500 nm; medium if at least one dimension > 500 nm; large if at least one dimension > 1000 nm); numerical values from Williamson-Hall analysis (HR-XRD data): in blue the estimated length along (hk0), in orange the estimated length along (00 l); the indicated maximum is 1000 nm, apart from larger particles (i.e., *KF Chemicals*; *VM cachet bleu, blanc et or*; *Lefranc paint tube*)

^f *Vieille Montagne*

^g 73.9 wt% Zn calculated by PIXE. XRD and FTIR revealed that the sample is mostly made of hydrozincite

Inorganic phase(s) of zinc white materials

The inorganic phases of the samples were studied using a combination of results from PIXE and XRD analyses. PIXE measurements were used to quantify the amount of the significant mineral phases composing the samples and trace elements. The results were expressed in weight

percent (wt%). XRD allowed the identification of the crystalline phases of the samples.

Purity and formulations of zinc white materials The amount of ZnO (in wt%) detected for each sample investigated by PIXE is indicated in Table 3.

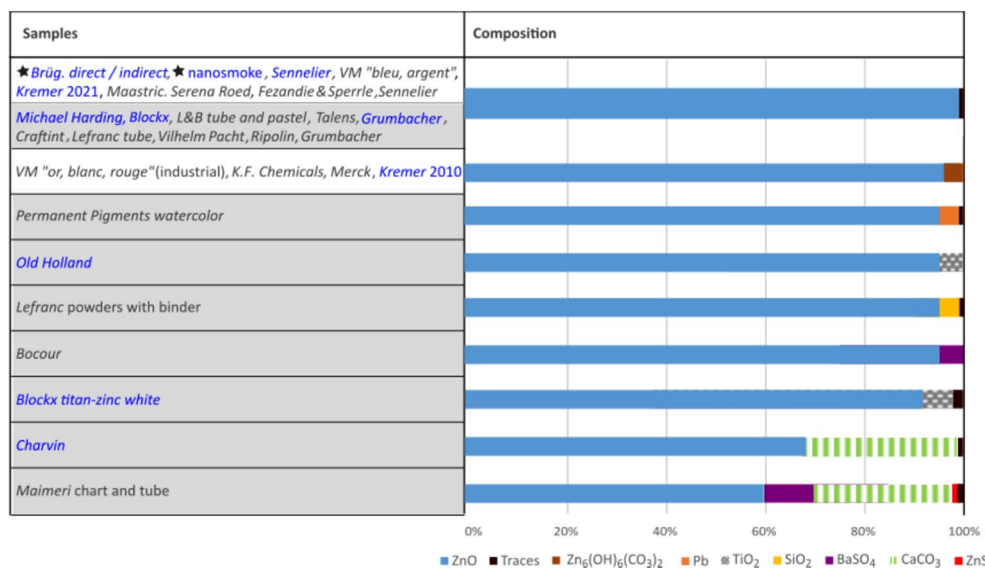


Fig. 2 Composition of the zinc white samples belonging to the corpus of the study. Reference samples are indicated with a star; in blue are modern samples, and in black are historical ones. White background for samples in the form of powder, gray for samples in the form of paint

As shown in Fig. 2, most of the analyzed samples were almost pure ZnO (>98 wt%), in particular the powder samples (including the three reference materials).

The only exceptions were ten powders containing hydrozincite ($\text{Zn}_5(\text{CO}_3)_2(\text{OH})_6$), identified by XRD¹⁰ and FTIR. In particular, the compound was found in the 2010 Kremer ZnO powder, while it was not detected on the very same powder back in 2010 with the same setup; the Kremer ZnO powder purchased in 2021 did not contain hydrozincite either. These results suggest that the compound formed over time, probably from converting ZnO upon exposure to air [38, 63]. Interestingly, it was found only in industrial *Vieille Montagne* samples, not in the ones referred to by the company as “lab samples”.

The *Sikkens* powder, mostly hydrozincite with some lead-based compound and likely some ZnO, represents a peculiar case. An FTIR spectrum of the sample is available in the Additional file 1: Figure S1.

Over half of the paint samples were almost exclusively made of ZnO (>98 wt%, Fig. 2, Table 3). Though usually not mentioned on the product label, the rest of the corpus contained significant amounts of other compounds (4–35 wt%) such as titanium dioxide (TiO_2), calcium carbonate (CaCO_3), barium sulfate (BaSO_4), quartz (SiO_2) and lead-based compounds (Fig. 2).

Interestingly, four samples branded as zinc white¹¹ proved to be made out of entirely other compounds than ZnO. This is possibly evidence of adulteration, a common issue for artists' materials, particularly zinc white, in the 19th century, as the recurrence of the topic in painting treatises of the time shows [64, 65]. Those samples, listed at the bottom of Table 3, were not investigated further in this study; only the *Sikkens* powder mentioned above was investigated further due to the detection of hydrozincite.

Trace elements Several elements were detected as traces (<1 wt%) by PIXE in both powders and paints: iron, nickel, lead, sulfur, calcium, aluminum, chlorine, silicon, titanium, strontium, potassium, zirconium, magnesium, tin, and cadmium (Fig. 3).

Iron and nickel were detected in almost all samples, with values usually lower than 0.1 wt%. Iron is likely ascribed to contamination, while the detection of nickel may be related to the PIXE detector. Lead and sulfur were present in about half of the analyzed samples, almost exclusively historical; calcium, aluminum, and chlorine were found in about a third of the analyzed samples, mostly paint materials, while others were found sporadically. For example, cadmium traces were detected only in the *Fezandie & Sperrle* zinc white powder and might be related to European zinc ores, as underlined by Holley [66].

¹⁰ HR-XRD used for the quantification, when available.

¹¹ A *Blockx* paint tube, lead-based; *Sikkens* powders, mostly made of hydrozincite with ZnO and some lead-based minor compound; *Permanent Pigments* powders, titanium white; a titanium-zinc white jar, a mixture of CaCO_3 , BaSO_4 , TiO_2 , quartz with ZnS and ZnO as minor compounds.

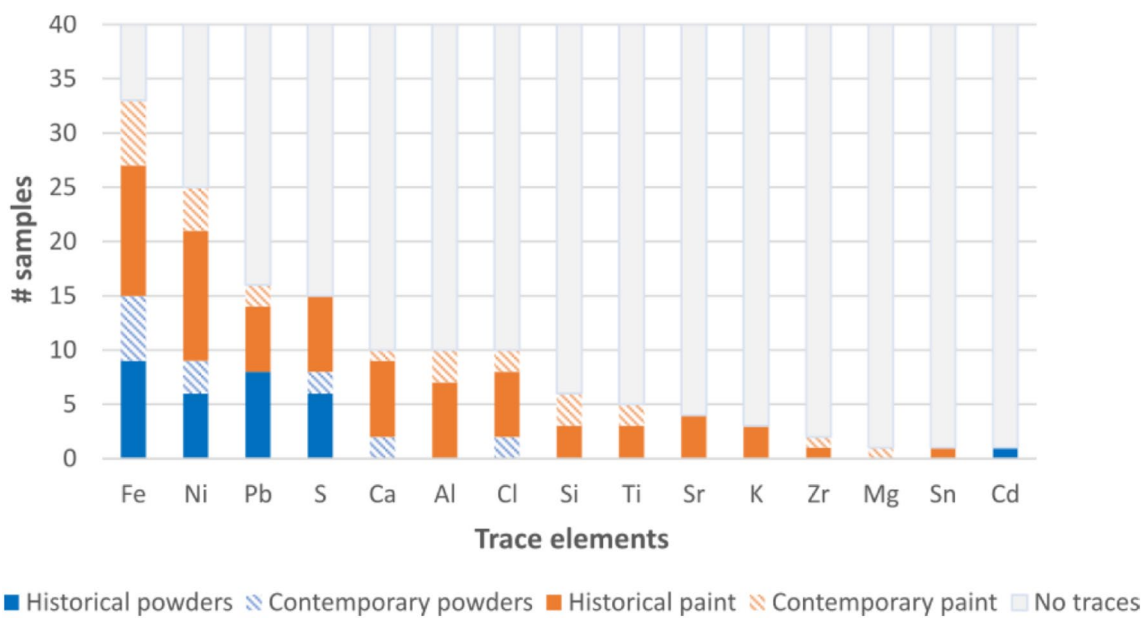


Fig. 3 Trace elements in zinc white samples belonging to the corpus of the study analyzed by PIXE

Looking at reference samples, *Brüggemann* indirect and ZnO nanosmoke powders were the purest of the corpus, with no traces other than iron and nickel (about 200–500 ppm in total). *Brüggemann* direct ZnO was less pure regarding amount (~3200 ppm) and type of trace elements (i.e., sulfur, chlorine, calcium, and iron). The *Sennelier* powder stood for its extreme purity (less than 2000 ppm of trace elements).

Some trace elements were only detected in paint materials (i.e., aluminum, silicon, titanium, strontium, potassium, zirconium, magnesium, and tin; Fig. 3). Aluminum may come from aluminum stearates, a standard paint stabilizer, or aluminum silicates when detected with silicon (i.e., *Grumbacher*, *Vilhelm Pacht*, *Old Holland*, *Blockx* Ti-Zn white). Strontium likely originated from calcium carbonate or barium sulfate since it is a common impurity of the natural form of barium sulfate [1, 67] and was only detected in samples containing these compounds (e.g., *Maimeri*). Magnesium might come from magnesium carbonate, another standard filler [68]. The tin may be a residue from paint tubes made of this material since it was found only in the *Vilhelm Pacht* sample, dating back to before 1909. Moreover, iron was detected by SEM-EDX only in a grain of the *Grumbacher* pre-tested, which might support the abovementioned hypothesis that links this element to contamination.

Finally, results obtained by PIXE and SEM-EDX generally agreed, with a few exceptions. The latter technique did not detect certain trace elements (e.g., only zinc was detected in *Vilhelm Pacht*, *Crafint*, and *Grumbacher* 1950s paint tubes). In other cases, such as the *Bocour* (Ba, S and Ca, Mg, S in some grains) and *Lefranc & Bourgeois*

(Ca, S in some grains) tubes, some elements were only detected by SEM-EDX. The spots analyzed through the two techniques may have been locally richer in some compounds (e.g., driers, additives) due to the complexity and inhomogeneity of their formulations.

Particle morphology and size

This section is dedicated to the characterization of morphology and size of ZnO particles based on SEM observations. A classification upon Williamson-Hall analysis of HR-XRD data for a selection of samples is also presented. Results for reference materials are presented first, followed by results on the rest of the corpus.

Reference samples

The two *Brüggemann* reference samples produced by indirect and direct processes presented particles of distinct size and morphology (Fig. 4):

- ZnO produced by the indirect method had prismatic particles with hexagonal bases 40–400 nm wide (width W, in red) and 40–500 nm long (length L, in blue), as schematized in Fig. 4c;
- ZnO produced by the direct method had mostly acicular particles (i.e., tetrapod-arms grown from a common core), 60–1250 nm wide and 300–5800 nm long, as defined in Fig. 4d.

The third reference, the synthesized ZnO nanosmoke, exhibited tetrapod-like morphology, similar to the direct

method ZnO, but at the nanoscale (width < 50 nm, length > 100 nm) [49, 69].

The impact of the binder on the characterization of ZnO particle morphology and size was investigated for a couple of powders by comparing them *as-is* and ground in linseed oil. As shown in Fig. 5 for *Brüggemann* indirect ZnO powder and the corresponding paint mockup, the size of the particles is comparable.

Zinc white samples of the corpus

Powders and paint materials mainly showed prismoidal morphology (Table 4, Fig. 6a), like the *Brüggemann* indirect ZnO powder. However, particles with acicular morphology were also observed in some samples, such as the *Vieille Montagne* powders¹² (Fig. 6b) and *Ripolin* and *Talens* paint materials.

All the samples were quite heterogeneous in size, as shown in Fig. 6c (*Talens* paint tube).

An overview of the observations is provided in Table 3; detailed results are in Additional file 2: Table S2.2. Our findings agree with Johnson's observations [9], who noted their consistency with the optimal particle range of 0.2–0.8 μm for paint opacity, durability, and gloss.

Since it was not possible to unequivocally classify the samples based on SEM images, in-depth diffraction studies were performed at the synchrotron radiation facility ESRF in Grenoble (France) to estimate the apparent size, aspect ratio, and strain of the ZnO crystallites. The results of the Williamson-Hall analysis are shown in Fig. 7, where the length along the direction (00 l) has been plotted against the length along (hk0). The values were calculated as described in the Additional file 1.

Figure 7 shows two clusters of samples, with decreasing sizes for the most recent ones (in blue). *Vieille Montagne* and *Lefranc* samples are all larger than one micrometer. In this cluster is also the *Vilhelm Pacht* tube, which dates back to the end of the 19th/beginning of the 20th century. Moreover, samples presenting prismoidal and acicular morphologies had generally larger crystallites (framed in red in Fig. 7). The smaller particles (< 600 nm) cluster included the most recent *Lefranc & Bourgeois* samples, the *Sennelier* historical powder, and 20th-century samples like the *Maimeri* color chart and paint tube.

Results from the Williamson-Hall analysis were generally coherent with SEM observations, but in some cases, the method overestimated¹³ or underestimated¹⁴ the size

of some particles compared to SEM. In particular, *Brüggemann* direct ZnO powder and the *Talens* pristine paint tube presented larger particles in SEM images than the values estimated by Williamson-Hall analysis (Table 3; Additional file 2: Table S2). This shows the limitations of the method, which is unsuitable for assessing the size of crystallites larger than one micrometer and for samples with a broad size distribution. The estimated value is a non-weighted average that may not represent the size distribution. However, the method is still helpful for comparing samples, which is more complex through SEM images. These are high-magnification images of a specific sample area, which might not represent the whole sample. Moreover, it is hard to find a metric based on SEM images to compare samples to each other, especially with such a broad size distribution.

The Williamson-Hall analysis was also a valuable tool to classify paint samples where the ZnO particles were difficult to observe using SEM due to the presence of large agglomerates of particles (e.g., the dried yellowed *Talens* tube and the *Lefranc* powder with a binder).

By plotting the projection of the average sizes calculated for each peak over the perpendicular planes ab and bc, it was possible to visualize the crystal geometry of the analyzed samples, as shown in Fig. 8.

This provides a visual representation of the elongated morphology of ZnO particles (aspect ratio > 1) and of the larger crystallite sizes of historical materials, here represented by *Vieille Montagne* powders and a *Lefranc* 1930s paint tube (respectively in green, orange, and red in Fig. 8), compared to modern ones (in light and dark blue and black in Fig. 8). Moreover, the highest aspect ratio values were obtained for the synthesized ZnO nanosmoke (2.1) and *Vieille Montagne* and *Lefranc* samples (2.2–2.8), which might mirror the presence of acicular particles besides prismoidal ones.

Finally, the calculated strain coefficient was similar for all the analyzed samples (~ 0.01%), meaning that most differences in peaks broadening are related to size rather than strain effects.

A summary of the results of the Williamson-Hall analysis is available in Additional file 2: Table S2.3.

Luminescence

This section is dedicated to the luminescence of the analyzed samples. After a short introduction to the luminescence behavior of ZnO, results of the behavior under UV at optical microscopy will be presented, followed by observations at cathodoluminescence. Finally, findings from IBIL will be briefly presented.

Luminescence is strictly linked to the electronic structure of ZnO. In the case of perfect crystals, the radiative

¹² Except the *Vieille Montagne* "cachet argent" powder, which exhibited only prismoidal morphology.

¹³ Usually in terms of length for samples like *Fezandie & Sperrle* powder and *Lefranc & Bourgeois* paint tube.

¹⁴ Usually in terms of width for samples like *Vieille Montagne* and *Merck* powders.

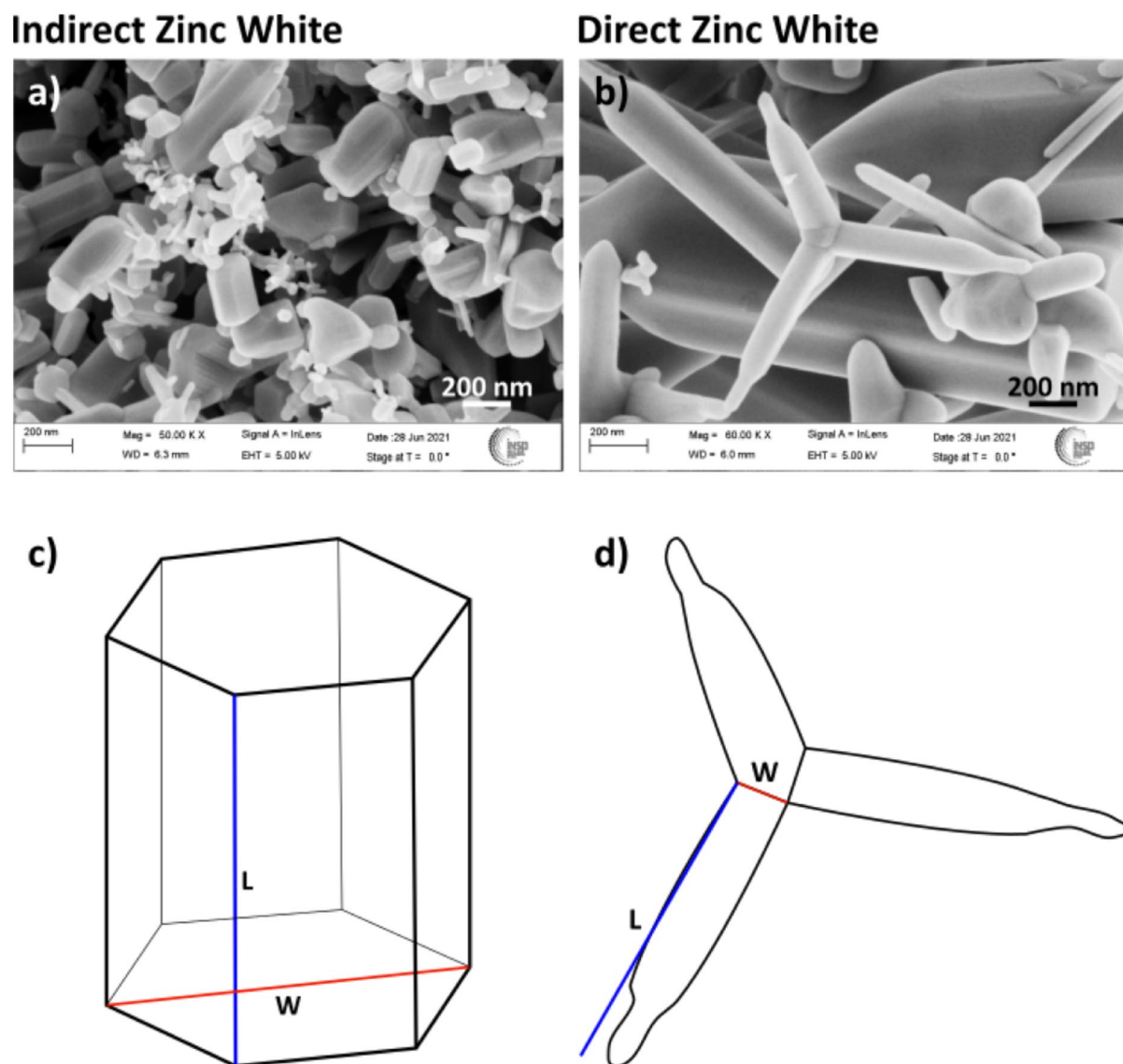


Fig. 4 SEM images (secondary electrons, 5 kV, working distance ~6 mm) of ZnO powders by Brüggemann (at the top): **a** indirect method; **b** direct method; schema of the main ZnO morphologies (at the bottom): **c** prismatic shape of hexagonal basis; **d** acicular shape. The length (L) and width (W) measured on SEM images are also indicated

recombination of excitons generated with excitation energy larger than the energy band gap (EBG) results in emission energy equal to the EBG, the so-called near band edge (NBE), or fundamental emission. However, when intrinsic or extrinsic defects are present, they create further energy levels within the band gap, available for excitons to recombine. This results in emission energies lower than the EBG. Therefore, the luminescence behavior directly measures crystal quality (i.e., the presence or absence of defects). The fundamental emission of ZnO is at ~3.2 eV (~390 nm); Zhang et al. [49, 69] attributed green photoluminescence (~530–590 nm) to oxygen

vacancies, blue/violet photoluminescence (~430 nm) to interstitial zinc (due to synthesis in non-equilibrium conditions and rapid quenching, which favors Zn-rich zinc oxide), and yellow photoluminescence (~600 nm) to interstitial oxygen-related species.

Photoluminescence under UV at the optical microscope

The three references presented two types of luminescence, blue or green, as illustrated in Fig. 9. Indirect ZnO had grains of weak blue luminescence under UV (Fig. 9a, b). In contrast, direct ZnO had a bright green luminescence (Fig. 9c, d), and ZnO nanosmoke an overall green

Powders

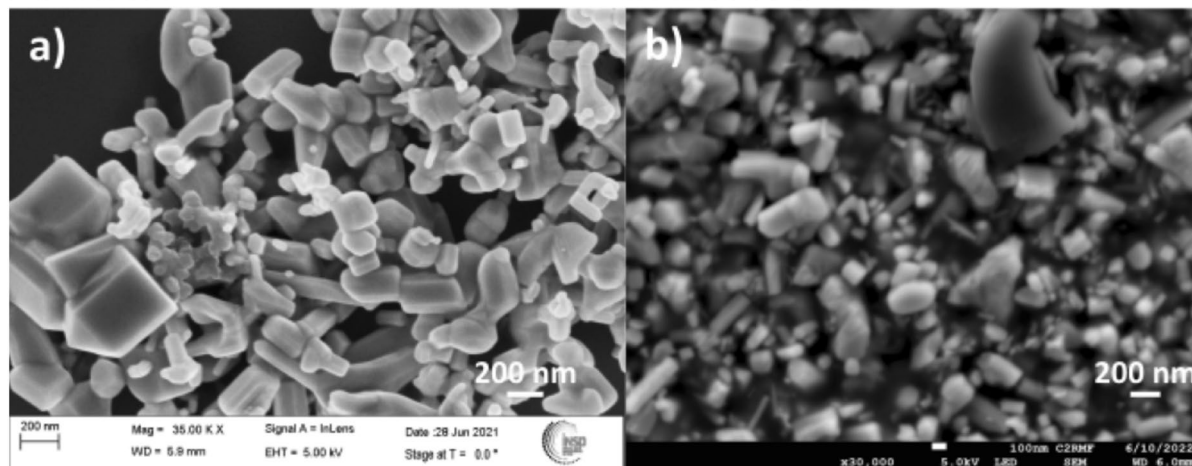


Fig. 5 SEM images (secondary electrons, 5 kV; working distance~6 mm) of ZnO powder by Brüggemann: **a** as-is; **b** ground in linseed oil

(but less bright) luminescence with blue-fluorescing areas (Fig. 9e, f).

The rest of the corpus presented blue, green, blue-green, or orange luminescence (Fig. 10).

All the powders and most paint samples presented green luminescence under UV, similar to the Brüggemann direct ZnO powders and the synthesized ZnO nanosmoke. About one-quarter of the paint samples exhibited blue luminescence similar to the Brüggemann indirect ZnO powders. Four paint samples had green-blue luminescence. Some samples presented luminescent grains of different colors and intensities, as shown in Additional file 2: Table S2.4.

Three samples, all from the Netherlands and containing hydrozincite, stood out from the corpus for their orange luminescence (Fig. 10c, d): these are all but one Maastrichtsche powder¹⁵ (i.e., *Serena Witzegel, Roedzegel n°1, Grijzegel n°3*). The same luminescence was observed on the *Sikkens* powder, mainly composed of hydrozincite.

Finally, bright blue luminescence was observed when ZnO nanosmoke was ground in linseed oil¹⁶ (Fig. 11).

Cathodoluminescence

The analyzed samples were classified based on the observed luminescence color, supported by the collected spectra (Figs. 12, 13). Additional file 2: Table S2.4 contains details about peak position and intensity.

Two types of luminescence were observed:

In linseed oil

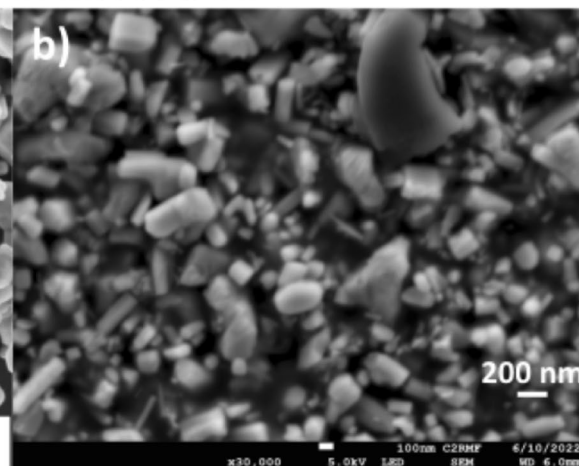


Table 4 Morphology of zinc white samples based on SEM observations

Samples	Morphology	
	Prismoidal	Acicular
★Brüggemann indirect, Fezandie & Sperrle, KF Chemicals, Kremer 2010 and 2021, Sennelier, Sennelier, VM "cachet argent"	✓	-
Bocour, Craftint, Grumbacher 1950s, Grumbacher pre-tested, Lefranc & Bourgeois, Maimeri tube, Ripolin, Vilhelm Pacht, Lefranc & Bourgeois tube	✓	-
★Brüggemann direct, Merck, VM "cachet bleu, blanc, or, rouge"	✓	✓
Ripolin, Talens	✓	✓
★ZnO nanosmoke	-	✓

Morphology of zinc white samples. Reference samples are indicated with a star. In blue modern samples, in black historical ones. White background for samples in form of powder, gray for samples in form of paint materials

- Blue luminescence, as for the ZnO produced by the indirect method and the synthesized ZnO nanosmoke (brighter than the previous one), with an intense peak at ~390 nm; the latter also presented a shoulder at ~430 nm and a larger band at ~530 nm (Fig. 12a, c);
- Green luminescence for ZnO produced by the direct method, with a large intense band at ~530 nm (Fig. 12b).

The peak at 390 nm will be indicated as NBE (Near Band Edge), and the large band at ~530 nm as GL (Green Luminescence).

The results obtained for the entire corpus are described in Table 5, compared to the luminescence observed under UV.

¹⁵ Maastrichtsche *Serena Roedzegel* did contain hydrozincite (detected by XRD and FTIR), but exhibited green luminescence.

¹⁶ The same results were observed when using two types of linseed oil.

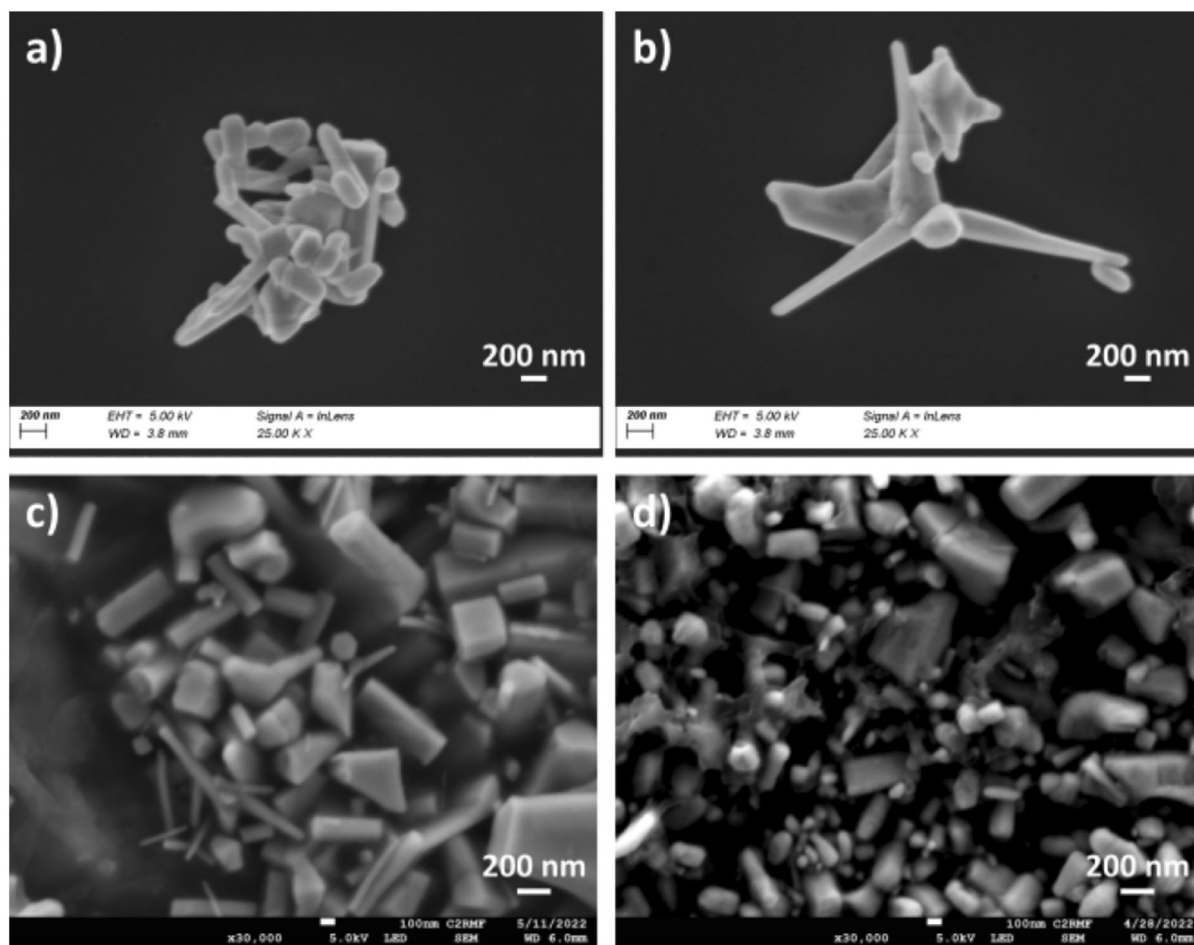


Fig. 6 SEM images (secondary electrons, 5 kV, working distance~6 mm) of **a–b** *Vieille Montagne* white seal ZnO powder; **c** *Talens* paint tube; **d** *Lefranc & Bourgeois* paint tube

All the samples in the form of powders exhibited green luminescence (Fig. 13a) except for *Kremer*, which was blue-fluorescing. On the other hand, paint tubes were mostly blue-luminescent (Fig. 13b), except for the green-luminescent *Lefranc*, *Ripolin*, and *Talens* samples. Blue-luminescent American paint tubes (i.e., *Grumbacher*, *Permanent Pigments*, *Bocour*) and the modern *Lefranc & Bourgeois* paint tube also had green-fluorescing grains, which would explain the appearance of the GL band in the corresponding spectra (Fig. 13c).

Green luminescence was generally more intense than blue luminescence; thus, exposure conditions had to be slightly adjusted for some samples, such as *Vieille Montagne*, *Sennelier*, direct ZnO powders, and *Talens* and *Craftint* paint tubes.

The color of the luminescence observed at cathodoluminescence did not always match that observed at OM under UV (Table 5), as in the case of ZnO nanosmoke (Fig. 14a, b), the *Talens* paint tube (Fig. 14c, d) and the Dutch powders.

Finally, the presence of a binder affected the intensity of the peaks but not their position, as shown on mockups prepared with *Brüggemann* indirect and direct ZnO and linseed oil (Fig. 15).

Ion beam-induced luminescence

IBIL analyses were also performed on the samples analyzed by PIXE. As for photoluminescence under UV, the general trend of IBIL results did not perfectly agree with CL findings. Additional file 2: Table S2.4 shows details about peak position and intensity.

Since the perceived color comes from the ratio of microscopic green and blue-fluorescing particles [9], these differences may arise from diverse sources: imperfect exposure conditions; inhomogeneity of some samples, especially paint tubes¹⁷; different excitation/

¹⁷ For example, the historical *Lefranc & Bourgeois* paint tube also contained Ca, Si, S, and P upon SEM-EDX point analyses. The fact that analyzing just a limited area of complex heterogeneous materials intrinsically presents the risk of not necessarily obtaining representative results.

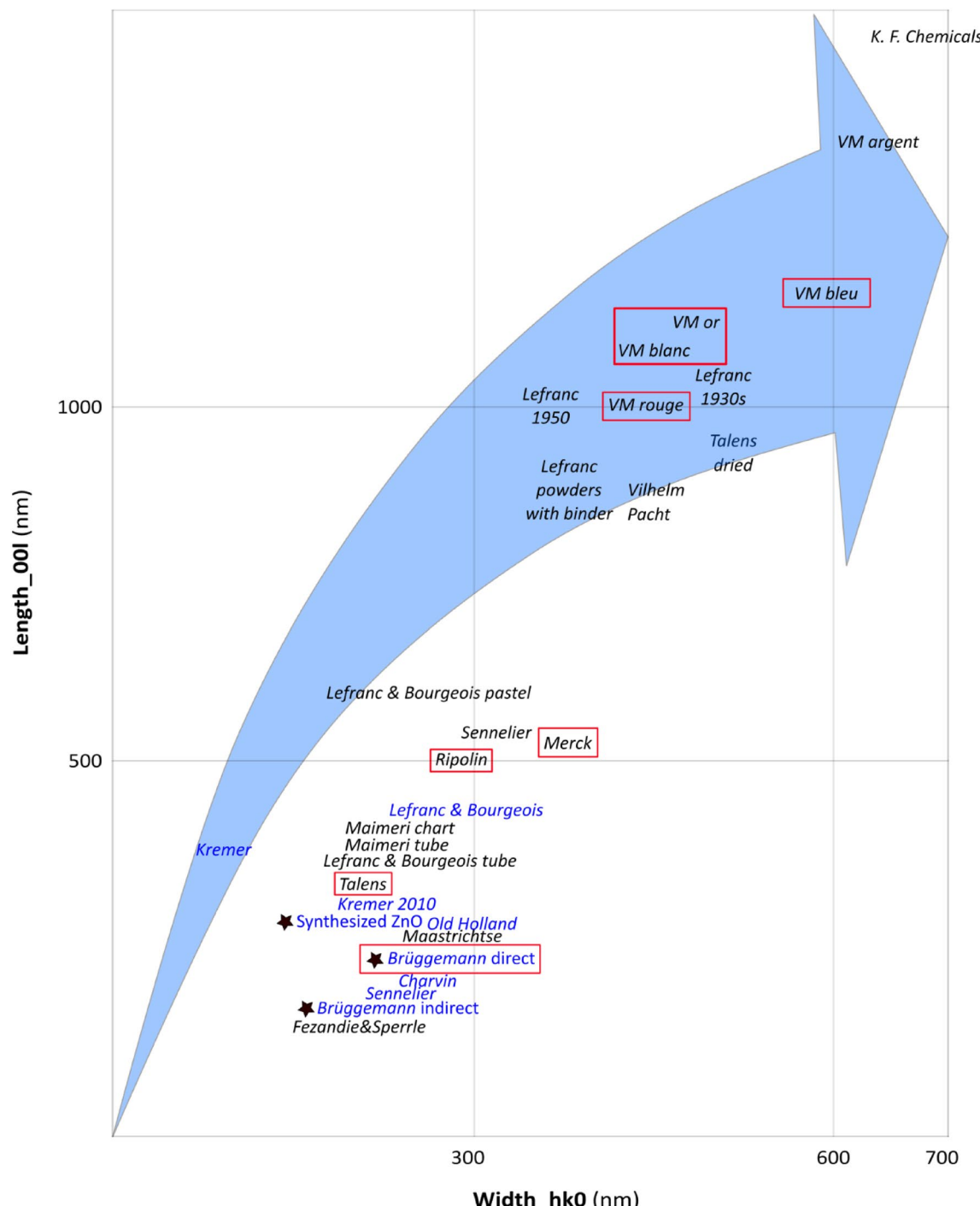


Fig. 7 Size trend of the samples based on results of the Williamson-Hall analysis. Reference samples are indicated with a star. In blue modern samples, in black historical ones. Framed in red are samples also containing acicular particles. Values larger than 1000 nm are not reliable anymore

emission paths¹⁸ induced by the various techniques; damage from high-energy radiation in ionoluminescence.

¹⁸ The width of the GL band varies compared to the NBE, which might suggest the presence of different defects.

The different excitation/emission paths may be explained by the fact that electrons and protons are massive and carry more momentum than photons; this may lead to different selection rules for cathodo- and ionoluminescence than UV-photoluminescence. The high

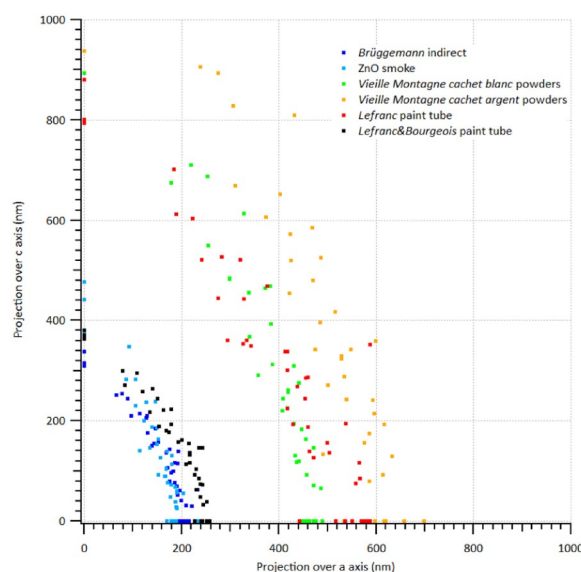


Fig. 8 Representation of the crystal geometry—(a*, c*) cross section of ZnO crystallites based on average crystal sizes computed by Williamson-Hall analysis of Brüggemann indirect ZnO powder (blue), ZnO nanosmoke powder (light blue), white seal Vieille Montagne ZnO powder (green), silver seal Vieille Montagne ZnO powder (orange), Lefranc 1930s paint tube (red), Lefranc & Bourgeois paint tube (black)

energy of electrons and protons may generate multiple excitation paths, resulting in relaxation pathways with corresponding cathodo- and ionoluminescence signatures different than those detected by photoluminescence. The higher energy of these particles may also lead to a more efficient excitation process, providing additional intermediate states.

Discussion

The discussion of the results is organized into four parts. Insights on colormen practices will be provided first. Then, our findings will be discussed to make a hypothesis on the synthesis process used to manufacture the samples, followed by the relevant trends found in the corpus with a focus on luminescence behavior.

ZnO manufacturers and colormen practices

The variety of brands forming the corpus allowed us to highlight some of their practices.

Concerning ZnO manufacturers, the comparison *Vieille Montagne-Maastrichtsche zinkwit Maatschappij* underlines the high purity of powders manufactured by the two companies, especially of the first. Purity is one of the main properties colormen look for in their raw materials. Thus, our findings on *Sennelier* and *Vieille Montagne* powders attested to the continuous high-quality

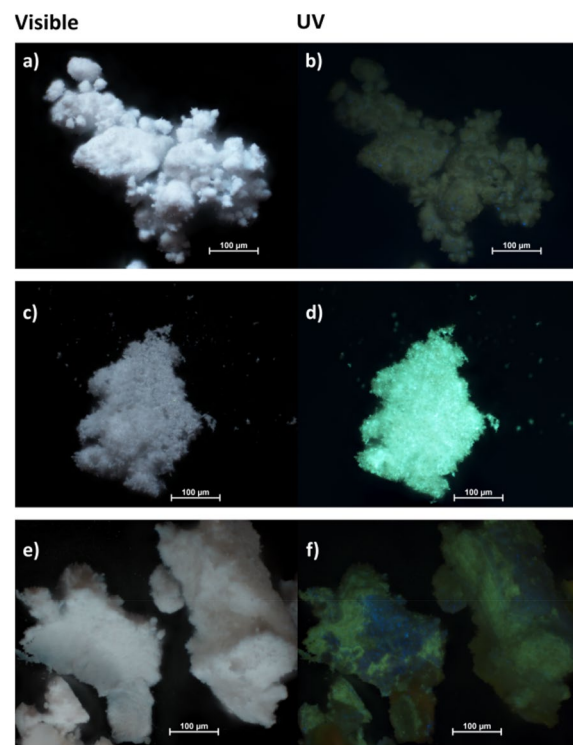


Fig. 9 Images at the OM (20x, under visible light on the left, under UV on the right) of the reference samples: **a–b** Brüggemann indirect ZnO; **c–d** Brüggemann direct ZnO; **e–f** ZnO nanosmoke

provisioning of the first and the purity of the products provided by the latter.¹⁹

However, the complex formulation of some paint tubes like *Sennelier's* and *Maimeri's* (Table 3; Additional file 2; Table S2) confirms the practice of mixing zinc white with other compounds such as barium sulfate [70], lithopone [71], calcium carbonate, zinc sulfide [38] or other pigments like titanium dioxide [72], to modify its optical and mechanical properties or to reduce costs. On the contrary, other paint samples, such as *Lefranc* and *Lefranc & Bourgeois*, did not contain any other compound than ZnO with a binder, coherently with the results of Casadio et al. [48] on an artist-grade *Lefranc* paint tube.

However, differences were observed even for the same manufacturer. The dried yellowed *Talens* paint tube presented larger particles than the pristine one. Did ZnO come from different batches of raw materials even though the tubes were sold in the same box?

Our results also provided information on possible adulteration due to the mismatch between products' labels and their actual content. This is relevant information to

¹⁹ *Sennelier* did buy ZnO from the *Vieille Montagne* at least during the first half of the 20th century. Personal communication.

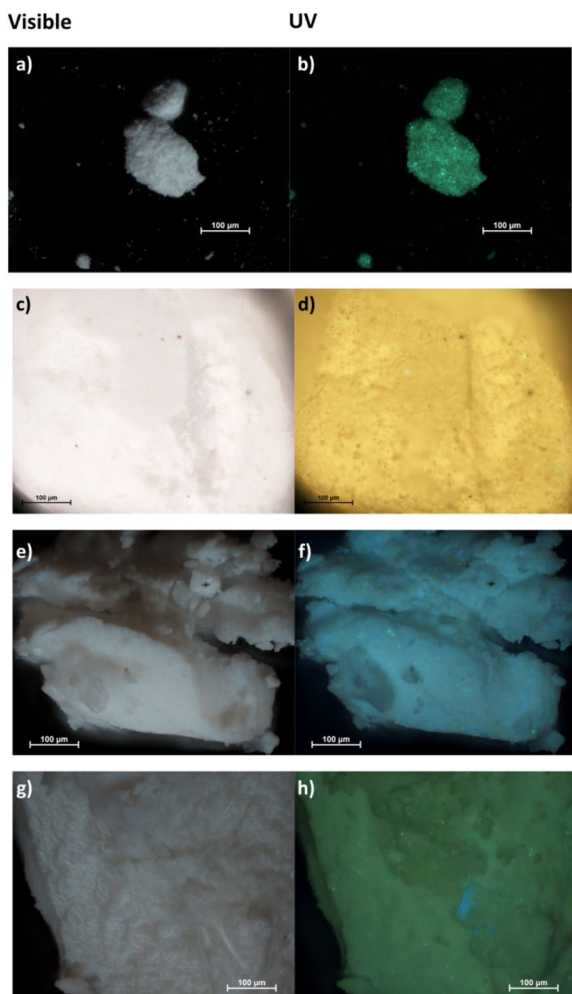


Fig. 10 Images at the OM (20x, under visible light at left and UV at right) of **a–b** Vieille Montagne white seal zinc white powder; **c–d** Maastrichtsche zinkwit mij. Ejsden zinc white powder, "Roodzegel n°1"; **e–f** Lefranc & Bourgeois zinc white contemporary paint tube; **g–h** Lefranc 1930s paint tube

consider for the analysis of artworks and the material history of paint materials.

Finally, modern formulations are not synonymous with more transparent labeling, as proved by the presence of unmentioned additives (10–35 wt%) in modern zinc white products (e.g., *Old Holland* and *Charvin* paint tubes).

The hypothesis of the indirect process

The findings for pigment powders matched the high purity standards for ZnO produced by the indirect method (i.e., ZnO>99 wt%) [1]. In the same way, the ZnO particles of the analyzed powders were similar to the ZnO indirect reference in terms of morphology and size. These results suggest that all the investigated

powder materials of the corpus might have been produced per indirect method, which is also supported by a historical booklet from *La Société Vieille Montagne*, stating that the company only made ZnO by indirect method to provide their customers with the purest products [73].

Properties trends

While composition, particle morphology and size, and historical sources pointed out the hypothesis of the indirect process, the observed green photo- and cathodoluminescence (i.e., wide, intense GL band at ~530 nm) of powders and most paint samples were not coherent with the results obtained for *Brüggemann* indirect ZnO (i.e., blue photo- and cathodoluminescence). Already Arte-sani et al. [39] associated samples with both blue- and green photoluminescence to the indirect method, thus to ZnO produced under a Zn vapor-rich environment or in non-equilibrium conditions (i.e., elevated pressure and temperature), for which interstitial zinc is the primary intrinsic defect [39], as found in ZnO nanosmoke [49]. Relying only on the NBE peak to identify zinc white may thus be misleading in some cases. The luminescence behavior will be discussed further in the next paragraph.

The second trend identified in the corpus consists of the smaller size of ZnO particles for the most recent samples. Results on *Vieille Montagne* materials support this hypothesis: while powders produced in the laboratory presented prismoidal submicrometer particles, the ones made at the *Valentin-Cocq* site had both prismoidal and acicular particles larger than one μm. Less controlled large-scale synthesis conditions may thus have affected their size. This means older samples produced via the indirect method might have larger particles and more defective structures because of poorly controlled synthesis conditions (i.e., growth time, temperature, and atmosphere). This would explain the corpus' significant size distribution, varied morphology, and luminescence behavior. Similar remarks were also reported by, for example, Hageraats et al. [25] and Capogrosso et al. [18] in some *Lefranc* samples.

As Zhang et al. [49, 69] showed, synthesis conditions are crucial in determining ZnO color and properties. The tetrapod-like ZnO nanosmoke used as a reference in this study can acquire hexagonal prism morphology if synthesized in an oxygen-rich atmosphere [69], the morphology most observed in the corpus. They also showed that Chemical Vapor Synthesis (i.e., dynamic conditions under gas flow, controlled temperature, and pressure) leads to smaller, more homogeneous particles (length<50 nm) [69]. This might prove the link of morphology and size of ZnO nanoparticles to oxygen pressure during synthesis or, more generally, to the control of synthesis conditions,

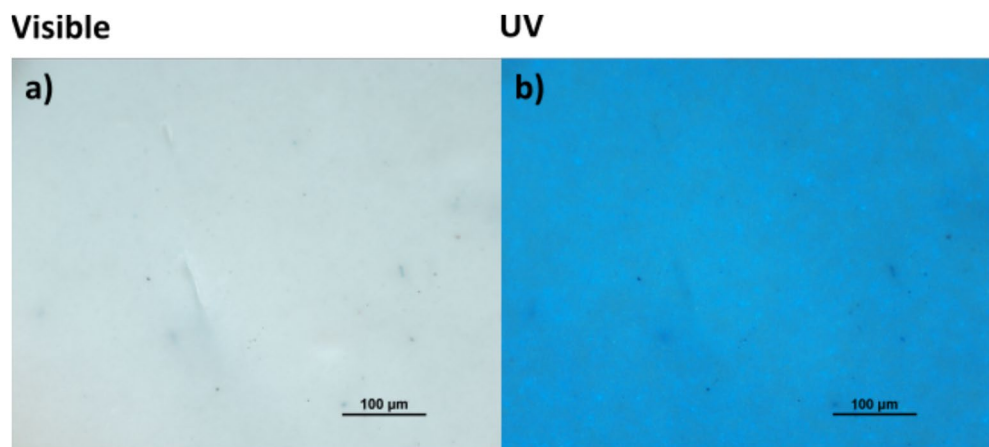


Fig. 11 Images at the OM (20x) of a paint mockup prepared with ZnO nanosmoke and linseed oil under **a** visible and **b** UV light

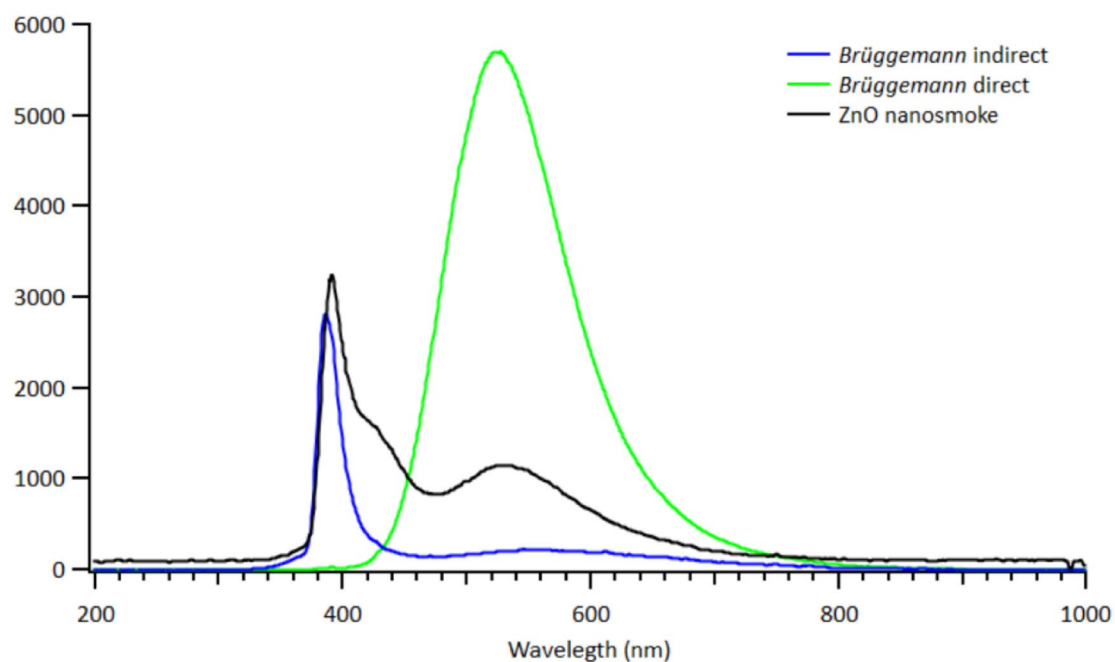
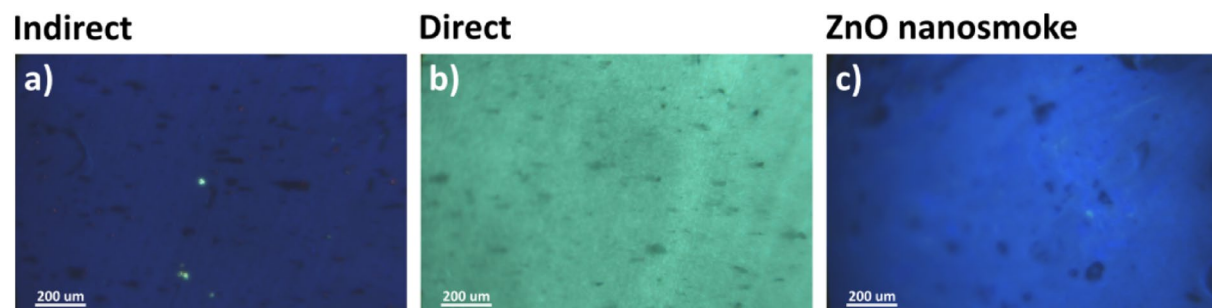


Fig. 12 Cathodoluminescence images (10x, ~390 μA, 11 kV; at the top) of: **a** Brüggemann indirect ZnO; **b** Brüggemann direct ZnO; **c** ZnO nanosmoke powders. The corresponding spectra are shown at the bottom of the Figure

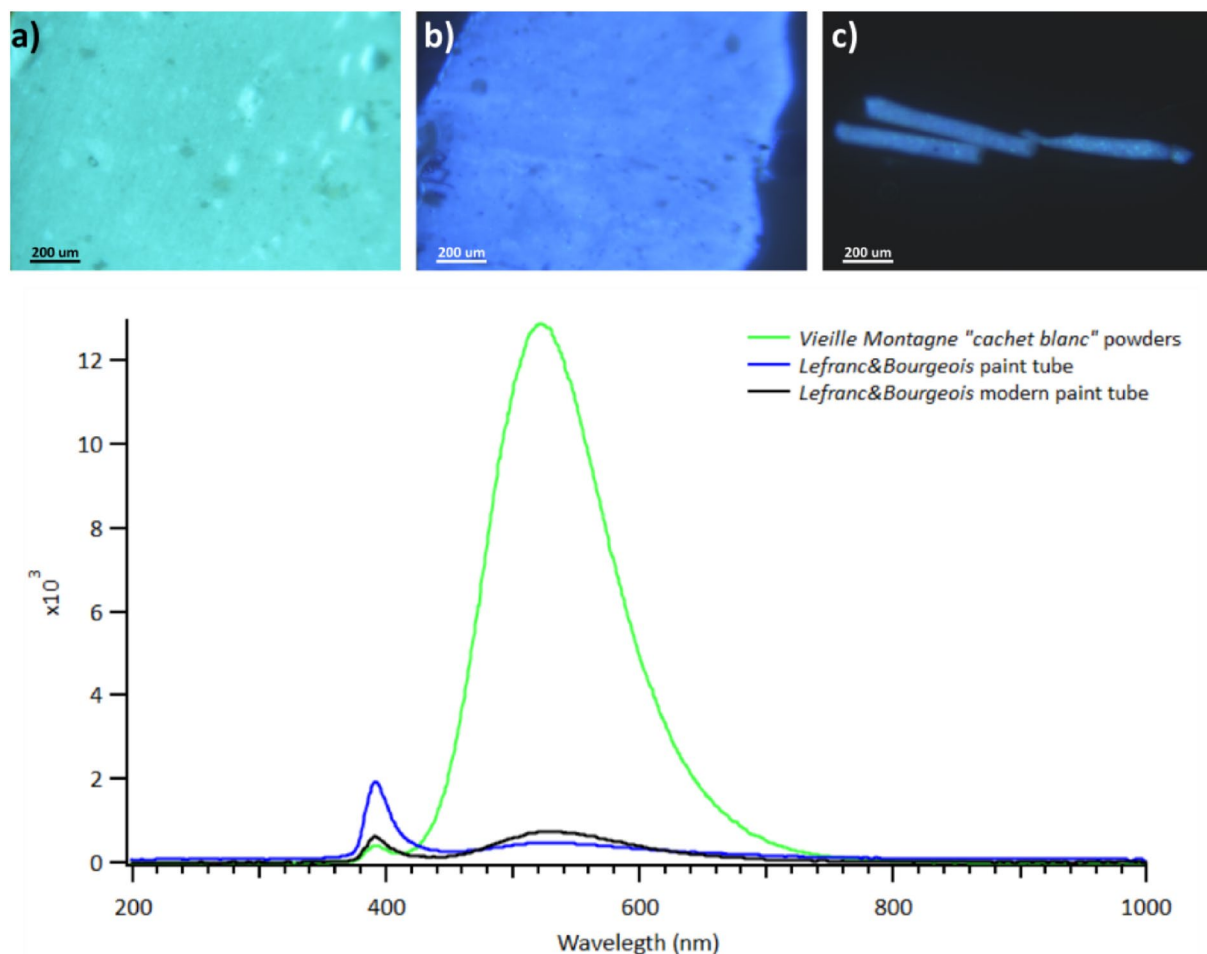


Fig. 13 Cathodoluminescence images (10x , $\sim 390 \mu\text{A}$, 11 kV ; at the top) of **a** Vieille Montagne white seal zinc white powders; **b** Lefranc & Bourgeois zinc white paint tube; **c** Lefranc & Bourgeois modern zinc white paint tube. The corresponding spectra are shown at the bottom of the Figure

which may have improved over time, leading to smaller particles of narrower size distribution.

A third trend concerns trace elements, possibly helpful in distinguishing historical from modern ZnO, at least for samples in the form of powders. While historical samples (e.g., *Vieille Montagne*, Dutch powders) consistently contained traces of lead and sulfur, modern ones included other elements like calcium and chlorine. This could be related to the fact that historical zinc white was likely produced using the same raw materials (i.e., zinc ores). In contrast, modern zinc white has a more complex supply chain, employing minerals from other parts of the world or recycled zinc, which could be contaminated.

Luminescence of zinc white

As mentioned above, luminescence was not directly correlated to other features of zinc white. Two hypotheses are presented here to describe the observed trends and their connection to other zinc white properties.

The NBE emission predominant in defect-free ZnO crystals was almost undetectable in some zinc white samples (i.e., *Vieille Montagne*, *Fezandie & Sperrle*, *Merck* powders; *Lefranc*, *Talens*, *Vilhelm Pacht* paint tubes). These were primarily historical materials with larger ZnO particles (Fig. 16), a trend already observed by Clementi et al. [36] in paint mockups.

Therefore, a first proposition correlates the GL to larger ZnO particles. Samples with larger particles and GL might once have had a less intense GL band, typical of the indirect method, and turned green-luminescent over time. Johnson [9] demonstrated that blue-fluorescing particles can shift to green-fluorescing particles over time via oxygen removal. Moreover, the role of oxygen on the luminescence behavior of ZnO was already highlighted by Morley-Smith [37], who observed a relation between the GL and the ZnO particle size and related it to the oxygen at the surface of ZnO particles.

Table 5 Comparison of photoluminescence under UV and cathodoluminescence of zinc white samples

Samples	Under UV	CL
★ Brüggemann indirect	Blue	Blue
Lefranc & Bourgeois tube, Bocour Titan-zinc white		
Blockx, Maimeri color chart, Old Holland, ZnO nanosmoke mockups		Not performed
Kremer 2010 and 2021, ★ ZnO nanosmoke	Green	Blue
Lefranc & Bourgeois, Maimeri paint tube, Craftint, Grumbacher, Permanent Pigments watercolor		Green
★ Brüggemann direct, Fezandie & Sperrie, KE Chemicals, Merck, Semmelier, VM cachet or argent, blanc rouge et bleu		
Ripolin, Talens	Blue-green	
Maastrichtsche Serena roedzegeel		Not performed
Blockx ^a , Charvin, Grumbacher, Lefranc 1950, Lefranc powders with a binder, Lefranc & Bourgeois pastel, Michael Harding, Ripolin, Sennelier acrylics		
Vilhelm Pacht, Bocour, Talens dried	Blue-green	Blue
Lefranc 1930s		Green
Maastrichtsche Serena Griizegel n°3, Roodzegeel n°1, witzegeel	Orange ^b	Blue-green

Color of the luminescence under UV and at cathodoluminescence. Reference samples are indicated with a star. In blue modern samples, in black historical samples. Samples containing hydrozincite are underlined. White background for samples in form of powder, gray for samples in form of paint

^a Zinc white and titan-zinc white

^b The Sikkens powder made of hydrozincite also exhibited orange luminescence under UV light and blue luminescence at CL

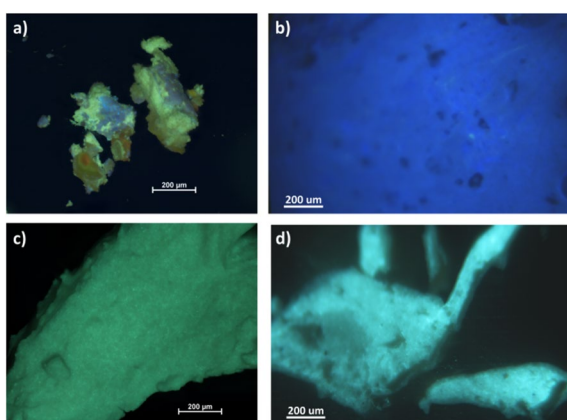


Fig. 14 Images at the OM (10x) under UV (on the left) and at cathodoluminescence (on the right) of **a, b** ZnO nanosmoke powders; **c, d** Talens paint tube

Zhang et al. [69] recently showed that the GL band indicates a more defective material rich in oxygen vacancies. However, they attributed their presence to the oxygen pressure conditions used in the synthesis rather than to the size and morphology of ZnO particles. This leads

to a second hypothesis: historical indirect ZnO with larger particles may exhibit more intense GL after manufacturing due to less controlled synthesis conditions.

The ratio of blue-to-green-fluorescing particles has been correlated to the photo-activity of ZnO, being higher for blue-fluorescing particles (e.g., higher chalking²⁰ rates observed for house paint) [9, 37], prevalent type in ZnO produced via the indirect method. To solve the issue, back in the 1950s, *Durham Chemicals* developed a ZnO indirect grade of larger green-luminescent particles (i.e., lower oil absorption and reactivity, higher reducing power) that could resist chalking [20], which proves the existence of different types of indirect ZnO. Hageraats et al. [74] also observed different types of zinc white in painting materials. This information is particularly relevant in light of the results of Hermans et al. [35], for example, who showed that zinc whites of different reactivity can be observed in paintings and potentially affect paint performance, especially in certain environmental conditions, such as upon use of solvents for conservation treatments, which are a trigger for the crystallization of zinc soaps. Moreover, most documented cases of severe degradation due to zinc white involve 20th-century rather than 19th-century artworks [23, 27, 75]; however, this may not be representative of the use and degradation of zinc white, since the pigment may have been employed more extensively from the end of the 19th century.

Nevertheless, it is essential to consider other factors, such as pigment-binder interaction, aging, and the presence of other compounds. In our corpus, barium sulfate—either alone (e.g., *Bocour* paint tube) or with calcium carbonate and zinc sulfide (e.g., *Maimeri* paint tube)—did not modify the cathodoluminescence response of ZnO samples. Hydrozincite did not seem to affect color and spectral features observed at cathodoluminescence either (e.g., in *Kremer* powders, which both presented bluish CL with no other spectral characteristics). Still, it might have played a role in the orange luminescence observed at the OM under UV light for some Dutch powders since all the samples exhibiting an orange luminescence under UV contained this compound (Table 5). Hydrozincite might affect the photoluminescence of zinc white only when present above a specific concentration since other ZnO samples containing some hydrozincite presented green luminescence (e.g., *Maastrichtsche Serena Roedzegeel* powder). However, the contribution of other compounds to the photoluminescence response of these samples cannot be excluded either. Further studies on these materials and hydrozincite will be performed to confirm these preliminary hypotheses on the orange photoluminescence.

²⁰ A result of the oxidation of the binder due to peroxides formation.

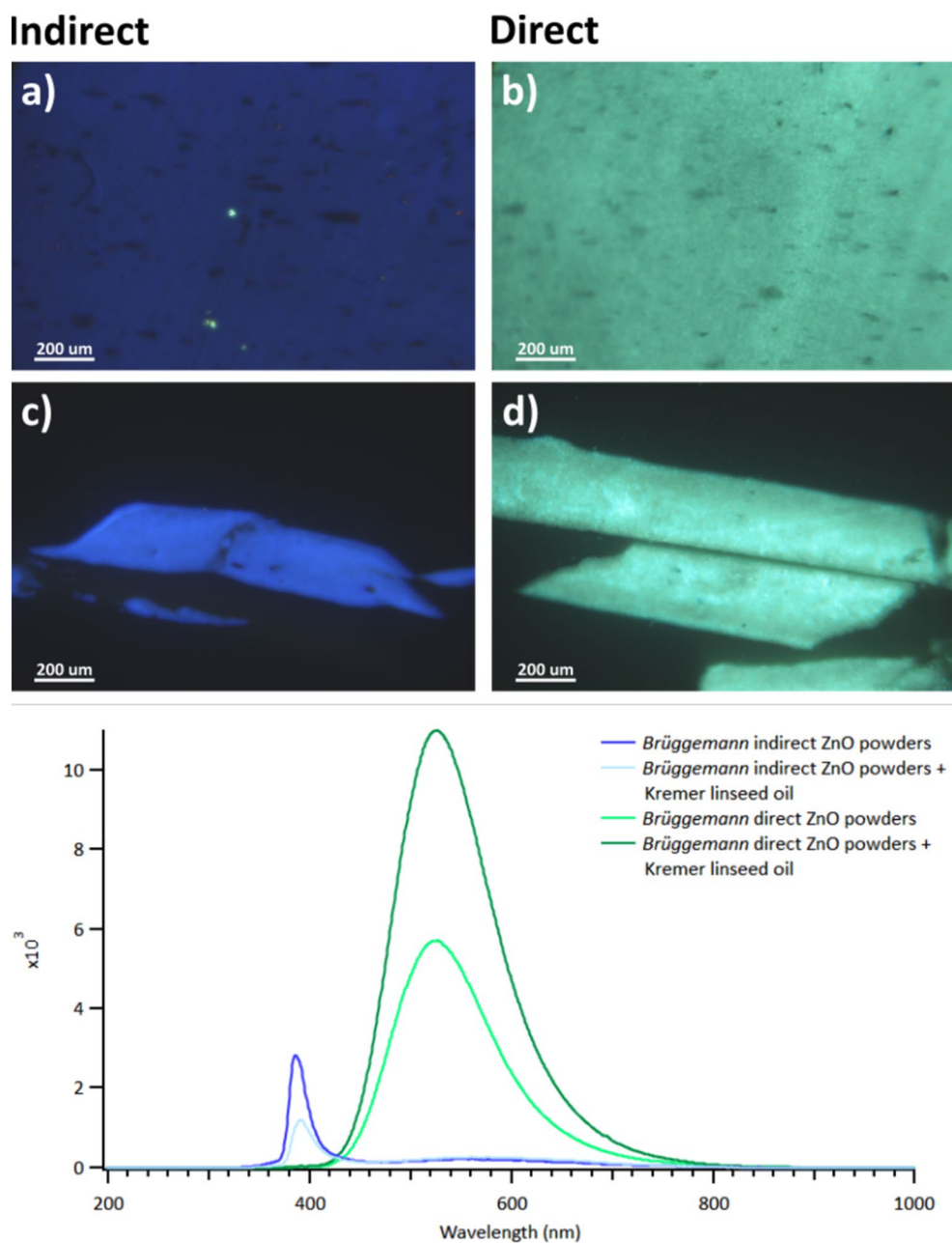


Fig. 15 Cathodoluminescence images (10x) and spectra of Brüggemann of **a** indirect ZnO powder; **b** direct ZnO powder; **c** indirect ZnO powder ground in linseed oil; **d** direct ZnO powder ground in linseed oil

Finally, optical cathodoluminescence, a technique widely used in geology [76], more rarely to study paint materials [77–79], proved an appropriate, easy-to-handle tool for identifying zinc white vs. other whites and zinc-based pigments. Our results add up to the research of Palamara et al. [77], the only systematic study of white pigments by cathodoluminescence presented until now, to the authors' knowledge. They showed applications of

SEM-CL aimed at building a database of the behavior of pigments at cathodoluminescence. In a complementary way, our study demonstrates a more accessible method to assess chemical differences through visual information (i.e., a large field image at the OM) and spectral features (spectroscopy). Once further reference databases are developed, the method could be of great value, especially

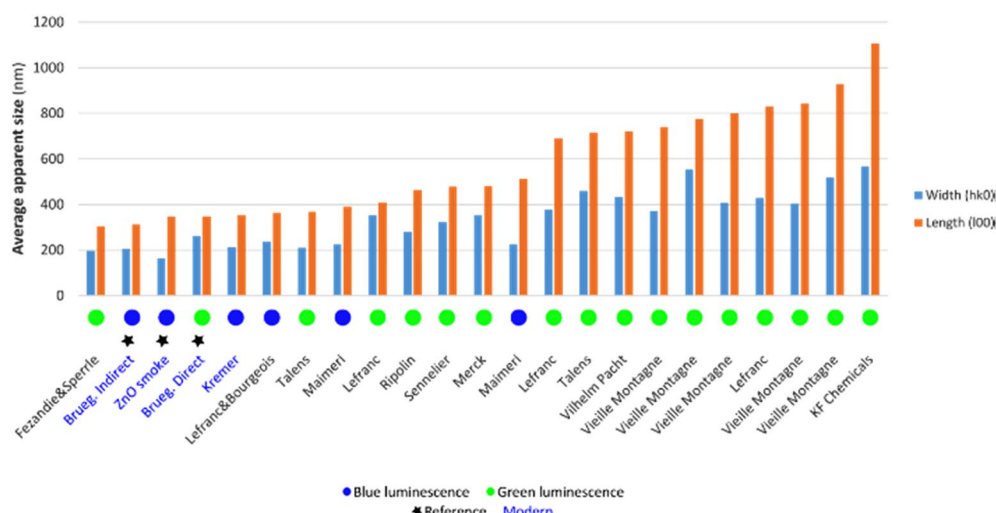


Fig. 16 Size trend of samples analyzed at the ESRF (Williamson-Hall analysis) classified by growing size along the (l00) direction (in orange). In comparison, the direction (hk0) is also shown (in blue). With a star are indicated reference samples, in blue are modern samples, and in black are historical ones. Green and blue dots indicate the color observed using cathodoluminescence

in distinguishing zinc white from other zinc-based pigments (e.g., lithopone, cobalt green, and zinc yellow).

Conclusions

The study of a unique, varied corpus of historical and modern zinc white artists' materials provided information on the variability of the properties of the pigment and colormen practices for zinc white formulations. The corpus presented some unavoidable biases and intrinsic limitations but still represents a good reference of zinc white properties for Heritage professionals.

Common additives, proportions, and combinations were identified for various color manufacturers and compared to their labeling, providing information about zinc white materials, their properties, and possible manufacturers' and artists' choices.

Hydrozincite was detected in some ZnO powders, even as the main component in the *Sikkens* powder; it was not found in any paint sample. The compound is likely a degradation product formed over time in powders exposed to air. It was identified by XRD and FTIR, which have different sensibilities to the compound but provide coherent results. In our corpus, the presence of hydrozincite had no impact on the cathodoluminescence response of ZnO samples, but it might be a cause of the orange luminescence observed under UV. Further studies are required to confirm if hydrozincite or other compounds are responsible for this behavior. Since crystallographic research on hydrozincite has not been published since the 1960s, the compound will be the object of another study.

The results for indirect and direct ZnO references agreed with the literature. The samples' high purity (i.e., a reduced amount and type of trace elements), prismoidal morphology, and submicron particle size match the characteristics of the ZnO synthesized via the indirect method. Acicular particles were sometimes observed in historical samples in addition to prismoidal ones, with a large particle size distribution for the whole corpus.

The luminescence behavior was indeed not straightforward to interpret. Both blue- and green-fluorescent materials were observed. The Near-Band-Edge peak at ~ 390 nm was not always detectable, even in pure historical powders without binders. This raises questions on the practical use of this feature for identifying zinc white. We formulated two hypotheses to explain that either blue-luminescent particles might have turned green-luminescent over time or some (less controlled) synthesis conditions promoted the formation of larger green-luminescent particles.

Modern materials had smaller ZnO particles than historical ones, containing some recurring trace elements, such as lead and sulfur.

Photo-, cathodo- and ionoluminescence results did not perfectly match. Cathodoluminescence proved a valuable complementary tool for studying pigments and paint materials. To the authors' knowledge, this technique, combined with optical microscopy, was used for the first time on such a large corpus of paint materials. Photoluminescence seems more sensitive than cathodoluminescence to the presence of compounds other than ZnO (e.g., probably hydrozincite), so comparing the two

techniques can be informative of compositional variations of the sample.

This study represents a solid database in which synthesis routes, intrinsic properties, and luminescence behavior of zinc white were discussed as a guideline for identifying and classifying zinc white. The presented findings will be used as a reference to study samples and cross-sections from 19th–20th century paintings to survey the extent and modalities of the use of zinc white, its properties, and its relation to painting degradation.

Archival and historical research on zinc white, its production, and use among 19th and 20th centuries color-makers, merchants, and artists will be deepened in an art historical review [80].

Abbreviations

CL	Cathodoluminescence
C2RMF	Centre de Recherche et Restauration des Musées de France
EBG	Energy Band Gap
ESRF	European Synchrotron Radiation Facility
GL	Green Luminescence
HR-XRD	High angular Resolution-X-Ray Diffraction
IBIL	Ion Beam-Induced luminescence
INSP	Institut de NanoSciences de Paris
IPANEMA	Laboratoire Institut Photonique d'Analyse Non-destructive Européen des Matériaux Anciens
OM	Optical Microscopy
NBE	Near Band Edge
PIXE	Particle-Induced X-ray Emission spectroscopy
PL	Photoluminescence
RCE	Rijksdienst voor het Cultureel Erfgoed (Cultural Heritage Agency of the Netherlands)
SEM-EDX	Scanning Electron Microscopy-Energy Dispersive X-ray spectroscopy
WH	Williamson-Hall
XRD	X-Ray Diffraction
XRF	X-Ray Fluorescence spectroscopy

Supplementary Information

The online version contains supplementary material available at <https://doi.org/10.1186/s40494-023-01082-4>.

Additional file 1: Table S1. Samples description. **Figure S1.** FTIR spectrum of Sikkens powders. PIXE fitting and Williamson-Hall analysis procedures.

Additional file 2: Table S2. Summary of the performed analysis.

Acknowledgements

This work benefited from State aid managed by the Agence Nationale de la Recherche (French National Research Agency) under the future investment programme integrated into France 2030, bearing the reference ANR-17-EURE-0021—Ecole Universitaire de Recherche Paris Seine—Foundation for Cultural Heritage Sciences. Financial support from the Access to Research Infrastructures activity in the Horizon 2020 Programme of the EU (IPERION HS Grant Agreement n.871034) is gratefully acknowledged. We thank Dr. Ineke Joosten, Prof. Klaas Jan van den Berg, and Rika Pause for their support during the ARCHLab access at the RCE. Samples from *Maastrichtsche zinkwit Maatschappij* and Sikkens were kindly provided through this access. We kindly acknowledge all the people and institutions that supported the presented study by providing some samples for building the *corpus* of analysis: *L. Brüggemann GmbH & Co. KG*, Salzstraße 131, 74076 Heilbronn, Germany (Mr. Markus Piotrowsky); *Maison de la Métallurgie et de l'Industrie de Liège*, Boulevard Raymond Poincaré

17, 4020 Liège (Ms. Elena Marcos Alvarez); Sidney and Lois Eskenazi Museum of Art at Indiana University (Ms. Julie Ribits); our colleagues Mr. Gilles Bastian and Ms. Nathalie Balcar from the C2RMF; the Art Materials Research and Study Center at the National Gallery of Art, Washington, D.C. 20565 (Ms. Tammy Hong and Ms. Kimberly Schenck); *Den Hirschsprungske Samling* and the Royal Danish Academy, Copenhagen, Denmark (Prof. Mikkel Scharff and Prof. Cecil Krarup Andersen); *Fondazione Maimeri* (Mr. Sandro Baroni and Ms. Maite Rossi); *Politechnico di Milano* (Prof. Daniela Comelli). The EQUIPEX NEW AGLAE research program (n. ANR-10-EQPX-22, French Ministry of Research) is acknowledged. This work was also carried out in the frame of the NewAGLAE project. We kindly acknowledge Ms. Maëva L'Héronde for her support with SEM images of ZnO powders at IPANEMA and Ms. Dominique Demaille for the SEM images of the reference ZnO powders at the INSP. We acknowledge the European Synchrotron Radiation Facility (ESRF) for providing synchrotron radiation facilities. We thank Dr. Catherine Dejoie for assistance and support using beamline ID22 and Dr. Marine Cotte, Dr. Victor Gonzalez, Dr. Letizia Monico, and Dr. Frederik Vanmeert for the BAG access. We thank the *Laboratoire d'Océanologie et de Géosciences* of the University of Lille for kindly allowing us to use their optical cathodoluminescence system for some samples of the corpus of study. We kindly acknowledge Prof. Didier Gourier and Dr. Thomas Calligaro for taking some time to discuss the luminescence of zinc white and Dr. Elyse Canosa for proofreading the English of the paper. Finally, we thank the reviewers for taking some of their precious time to read and provide their feedback on our work.

Author contributions

JS and NP conceptualized the study. NP and MO carried out SEM analysis. MO carried out OM and FTIR analysis and acquired CL spectra. NP acquired CL images. YC performed, supervised, and supported CL analysis. NP acquired PIXE/IBIL data, supported by QL and LP, for analysis and data treatment. NP acquired HR-XRD data. GW supported and supervised the treatment of HR-XRD data. SS and NP carried out the synthesis of ZnO nanoparticles. NP treated the data and prepared figures and tables. NP wrote the manuscript with the support of JS. MO participated in the writing of the draft. JS supervised the experimental work, contributed to the writing of the paper, and reviewed the manuscript in detail. VE provided advice on the general structure of the paper and reviewed the manuscript. GW, YC, SS, QL, and LP revised the paper, focusing on the parts related to their specific areas of expertise. NP, JS, YC, and SS worked on the review of the paper. All authors have read and agreed to the published version of the manuscript.

Funding

This work benefited from State aid managed by the Agence Nationale de la Recherche (French National Research Agency) under the future investment programme integrated into France 2030, bearing the reference ANR-17-EURE-0021—Ecole Universitaire de Recherche Paris Seine—Foundation for Cultural Heritage Sciences. Financial support by the Access to Research Infrastructures activity in the Horizon 2020 Programme of the EU (IPERION HS Grant Agreement n.871034) is gratefully acknowledged for the ARCHLab access at the RCE in Amsterdam.

Availability of data and materials

The datasets supporting the conclusions of this article are included within the article and in the Supplementary Materials.

Declarations

Competing interests

The authors declare no competing interests.

Received: 31 March 2023 Accepted: 6 November 2023

Published online: 07 February 2024

References

1. Kuhn H. Zinc white. In: Feller RL, editor. *Artists' pigments - a handbook of their history and characteristics*. London: National Gallery of Art, Washington Archetype Publications; 1986. p. 169–86.

2. Gardner HA. Paint researches and their practical application. Washington: Press of Judd & Detweiler, Incorporated; 1917.
3. Osmond G. Zinc white: a review of zinc oxide pigment properties and implications for stability in oil-based paintings. *AICCM Bull.* 2012;33(1):20–9.
4. Moezzi A, McDonagh AM, Cortie MB. Zinc oxide particles: synthesis, properties and applications. *Chem Eng J.* 2012;185–186:1–22.
5. Amir M, Abbas M, Fatima M, Khan ZS, Shah NA. Synthesis of carbon nanotubes and ZnO nanocomposites for IR sensing. *Appl Phys A.* 2021;127(11):882.
6. Zuliani A, Bandelli D, Chelazzi D, Giorgi R, Baglioni P. Environmentally friendly ZnO/Castor oil polyurethane composites for the gas-phase adsorption of acetic acid. *J Colloid Interface Sci.* 2022;614:451–9.
7. Flora RMN, Palani S, Sharmila J, Chamundeeswari M. Green synthesis and optimization of zinc oxide quantum dots using the Box-Behnken design, with anticancer activity against the MCF-7 cell line. *Appl Phys A.* 2022;128(4):359.
8. Tyagi N, Ashraf W, Mittal H, Fatima T, Khanuja M, Singh MK. A facile synthesis of ternary hybrid nanocomposite of WS₂/ZnO/PPy: An efficient photocatalyst for the degradation of chromium hexavalent. *Dyes Pigm.* 2023;210:110998.
9. Johnson VM. Ultraviolet-induced fluorescence and photo-degradation in zinc oxide watercolour paints. Doctoral thesis, Northumbria University. 2020.
10. Rogala D, Lake S, Maines C, Mecklenburg M. Condition problems related to zinc oxide underlayers: examination of selected abstract expressionist paintings from the collection of the Hirshhorn Museum and Sculpture Garden, Smithsonian Institution. *J Am Inst Conserv.* 2010;49(2):96–113.
11. Robb M. Ivan Le Lorraine Albright paints a picture. New York: ArtNews; 1950.
12. van Driel BA, van den Berg KJ, Gerretzen J, Dik J. The white of the 20th century: an explorative survey into Dutch modern art collections. *Herit Sci.* 2018;6(1):16.
13. Pergo F. Blanc de zinc (Zinc white) Le dictionnaire des matériaux du peintre (The painter's materials dictionary). Paris: Belin; 2005. p. 102–7.
14. Lefort MJ. Chimie des couleurs (Colors chemistry). Paris: French V. Masson; 1855.
15. Clarke M. A Nineteenth-Century Colourman's terminology. *Stud Conserv.* 2009;54(3):160–9.
16. Spennemann DHR. Stanislas Sorel's zinc-based paints. *Trans IMF.* 2020;98(1):8–13.
17. de Saint-Paul SG. Société Anonyme des mines et fonderies de zinc de la Vieille Montagne, 19 rue Richer Paris (Limited liability company Vieille Montagne - zinc miners and smelters), commercial catalog. Paris: Moulin; 1929.
18. Capogrossi V, Gabrieli F, Bellei S, Cartechini L, Cesariello A, Tricera N, Rosi F, Valentini G, Comelli D, Nevin A. An integrated approach based on micro-mapping analytical techniques for the detection of impurities in historical Zn-based white pigments. *J Anal At Spectrom.* 2015;30(3):828–38.
19. Eastaugh N, Nadolby J, Swiech W. Interpretation of documentary sources for the industrial preparation of zinc white in 19th century. In: Townsend JH, Nadolny J, Eyb-Green S, Neven S, Kroustallis S, editors. Dubois H. New York: Making and Transforming Art: Technology and Interpretation; 2014. p. 102–8.
20. Morley-Smith CT. The development of anti-chalking French process zinc oxide. *J Oil Colour Chem Assoc.* 1950;33:484–501.
21. Rogala DV. Everything old is new again: revisiting a historical symposium on zinc oxide paint films. In: Keune K, Noble P, Van Loon A, Hendriks E, Centeno SA, Osmond G, editors. Metal soaps in art: conservation and research. Cham: Springer; 2019. p. 317–30.
22. van den Berg KJ, Bonaduce I, Burnstock A, Ormsby B, Scharff M, Heydenreich G, Keune K, editors. Conservation of modern oil paintings. Cham: Springer International Publishing; 2019.
23. Casadio F, Keune K, Noble P, Van Loon A, Hendriks E, Centeno SA, Osmond G, editors. Metal soaps in art: conservation and research. Cham: Springer; 2019.
24. Sands S. Zinc oxide: warnings, cautions, and best practices. In: Just Paint. Published by Golden Artist Colors, Inc. 2018. <https://justpaint.org/zinc-oxide-warnings-cautions-and-best-practices/>. Accessed 19 Oct 2023.
25. Hageraats S, Keune K, Réfrégiers M, van Loon A, Berrie B, Thoury M. Synchrotron Deep-UV photoluminescence imaging for the submicrometer analysis of chemically altered zinc white oil paints. *Anal Chem.* 2019;91(23):14887–95.
26. Izzo FC, Kratter M, Nevin A, Zendri E. A critical review on the analysis of metal soaps in oil paintings. *ChemistryOpen.* 2021;10(9):904–21.
27. Andersen CK, Taube M, Vila A, Baadsgaard E. Zinc, Paint loss and Harmony in blue: degradation problems in Peder Severin Krøyer's paintings and the possible role of zinc white. *Perspective.* 2016; 1–16.
28. Osmond G, Keune K, Boon J. A study of zinc soap aggregates in a late 19th century painting by R.G. rivers at the Queensland art gallery. *AICCM Bull.* 2005;29:37–46.
29. Hermans JJ, Keune K, van Loon A, Stols M, Corkery RW, Iedema PD. The synthesis of new types of lead and zinc soaps: A source of information for the study of oil paint degradation. In: Bridgland J, editor, ICOM-CC 17th Triennial Conference preprints, Melbourne, 15 – 19 September 2014, art. 1603, International Council of Museums, Paris. 2014. p. 1–8.
30. Hermans JJ, Keune K, van Loon A, Iedema PD. An infrared spectroscopic study of the nature of zinc carboxylates in oil paintings. *J Anal At Spectrom.* 2015;30(7):1600–8.
31. Osmond G. Zinc white and the influence of paint composition for stability in oil based media. In: van den Berg KJ, Burnstock A, de Keijzer M, Krueger J, Learner T, Tagle A, Heydenreich G, editors. Issues in contemporary oil paint. Cham: Springer; 2014. p. 263–81.
32. Hermans JJ, Osmond G, van Loon A, Iedema P, Chapman R, Drennan J, Jack K, Rasch R, Morgan G, Zhang Z, Monteiro M, Keune K. Electron microscopy imaging of zinc soaps nucleation in oil paint. *Microsc Microanal.* 2018;24(3):318–22.
33. Baij L, Chassouant L, Hermans JJ, Keune K, Iedema PD. The concentration and origins of carboxylic acid groups in oil paint. *RSC Adv.* 2019;9(61):35559–64.
34. Hermans JJ, Helwig K. The identification of multiple crystalline zinc soap structures using infrared spectroscopy. *Appl Spectrosc.* 2020;74(12):1505–14.
35. Hermans JJ, Helwig K, Woutersen S, Keune K. Traces of water catalyze zinc soap crystallization in solvent-exposed oil paints. *Phys Chem Chem Phys.* 2023;25(7):5701–9.
36. Clementi C, Rosi F, Romani A, Vivani R, Brunetti BG, Miliani C. Photoluminescence properties of zinc oxide in paints: a study of the effect of self-absorption and passivation. *Appl Spectrosc.* 2012;66(10):1233–41.
37. Morley-Smith CT. Zinc oxide - a reactive pigment. *J Oil Col.* 1958;41:85–97.
38. Artesani A, Bellei S, Capogrossi V, Cesariello A, Mosca S, Nevin A, Valentini G, Comelli D. Photoluminescence properties of zinc white: an insight into its emission mechanisms through the study of historical artist materials. *Appl Phys A.* 2016;122(12):1053.
39. Artesani A, Dozzi MV, Toniolo L, Valentini G, Comelli D. Experimental study on the link between optical emission, crystal defects and photocatalytic activity of artist pigments based on zinc oxide. *Minerals.* 2020;10(12):1129.
40. Hageraats S. Developing microchemical imaging for the study of pigment degradation in oil paint. Doctoral thesis, University of Amsterdam. 2021.
41. Salvant Plisson J, de Viguerie L, Tahrouch L, Menu M, Ducoiret G. Rheology of white paints: how Van Gogh achieved his famous impasto. *Colloids Surf, A.* 2014;458:134–41.
42. Janas A, Mecklenburg MF, Fuster-López L, Kozłowski R, Kékicheff P, Favier D, Krarup Andersen C, Scharff M, Bratasz L. Shrinkage and mechanical properties of drying oil paints. *Heritage Science.* 2022;10(1):181.
43. Osmond G. Zinc oxide-centred deterioration of modern artists' oil paint and implications for the conservation of twentieth century paintings. Doctoral thesis, The University of Queensland. 2014.
44. Shimadzu Y, Keune K, van den Berg KJ, Boon JJ, Townsend JH, Boon JJ. The effects of lead and zinc white saponification on surface appearance. In: ICOM-CC 15th Triennial Meeting preprints volume II, New Delhi, 22–26 September 2008. Allied publishers. 2008. p. 626–632.
45. Nicolaus A. Réflexions sur le portrait dans l'œuvre de Hans Holbein le Jeune. Le "Portrait de la famille du peintre" des beaux-arts de Lille, copie ou réplique peinte sur parchemin de remplacement marouflé sur bois : propositions de conservation-restauration et d'une méthode d'analyse du support (Reflections on the portrait in the work of Hans Holbein the Young. The "Portrait of the painter's family" from the Lille Fine Arts Museum,

- copy or replica painted on replacement parchment mounted on wood: proposals for conservation-restoration and a method for analyzing the support). In French. Heritage Restorer Diploma-Painting Specialty, Institut National du Patrimoine, France. 2002.
46. Standeven HAL. Oil-based house paints from 1900 to 1960: an examination of their history and development, with particular reference to Ripolin enamels. *J Am Inst Conserv.* 2013;52(3):127–39.
 47. Kokkori M, Casadio F, Boon JJ. A comprehensive study of early 20th-century oil-based enamel paints: Integrating industrial technical literature and analytical data. In: Bridgland J, editor, ICOM-CC 17th Triennial Conference preprints, Melbourne, 15–19 September 2014, art. 0101, International Council of Museums, Paris. 2014. p. 1–8.
 48. Casadio F, Rose V. High-resolution fluorescence mapping of impurities in historical zinc oxide pigments: hard X-ray nanoprobe applications to the paints of Pablo Picasso. *Appl Phys A.* 2013;111(1):1–8.
 49. Zhang M, Averseng F, Haque F, Borghetti P, Krafft JM, Baptiste B, Costentin G, Stankic S. Defect-related multicolour emissions in ZnO smoke: from violet, over green to yellow. *Nanoscale.* 2019;11:5102–15.
 50. Otero V. Historically accurate reconstructions of Amadeo's chrome yellows: an integrated study of their manufacture and stability. Doctoral thesis, Universidade Nova de Lisboa. 2018.
 51. Christiansen MB, Baadsgaard E, Sanyova J, Simonsen KP. The artists' materials of P. S. Krøyer: an analytical study of the artist's paintings and tube colours by Raman, SEM-EDS and HPLC. *Heritage Sci.* 2017;5:39.
 52. Muir K, Langley A, Bezur A, Casadio F, Delaney J, Gautier G. Scientifically investigating Picasso's suspected use of Ripolin house paints in still life, 1922 and The Red Armchair, 1931. *J Am Inst Conserv.* 2013;52(3):156–72.
 53. Doherty S. Expand Your Options by Adding Zinc White Gouache to Transparent Watercolors. In: Artists Network. 2007. <https://www.artistsnetwork.com/art-mediums/mixed-media/expand-your-options-by-adding-zinc-white-gouache-to-transparent-watercolors/>. Accessed 19 Oct 2023.
 54. Richard P. Sennelier, l'artisan des couleurs (Sennelier, a history in color). In French/English. Editions du Chêne. 2012.
 55. Hopper E. Ledger books, record of the work of Edward Hopper. New York: Whitney Museum of American Art Books II-II; 1984.
 56. Pichon L, Calligaro T, Gonzalez V, Lemasson Q, Moignard B, Pacheco C. Implementation of ionoluminescence in the AGLAE scanning external microprobe. *Nucl Instrum Methods Phys Res, Sect B.* 2015;348:68–72.
 57. Altomare A, Corriero N, Cuocci C, Falcicchio A, Moliterni A, Rizzi R. QUALX2.0: a qualitative phase analysis software using the freely available database POW-COD. *J Appl Crystallogr.* 2015;48:598.
 58. Cotte M, Gonzalez V, Vanmeert F, Monico L, Dejoie C, Burghammer M, Hudler L, de Nolf W, Stuart F, Fazlic I, Chauffeton C, Wallez G, Jiménez N, Albert-Tortosa F, Salvadó N, Possenti E, Colombo C, Ghirardello M, Comelli D, Avranovich Clerici E, Vivani R, Romani A, Costantino C, Janssens K, Taniguchi Y, McCarthy J, Reichert H, Susini J, The, "Historical Materials BAG": a new facilitated access to synchrotron x-ray diffraction analyses for cultural heritage materials at the European synchrotron radiation facility. *Molecules.* 2022;27(6):1997.
 59. Chauffeton C, Costantino C, Iacconi C, Vanmeert F, Fazlic I, Monico L, Cotte M, Ghirardello M, Palladino N, Gonzalez V. Structural Analysis of Historical Materials. Eur Synchrotron Radiat Facil. 2024. <https://doi.org/10.15151/ESRF-ES-515931562>.
 60. Riminesi C, Villalobos Portillo EE, Possenti E, Beauvoit E, Avranovich Clerici E, Vanmeert F, Broers FTH. Structural Analysis of Historical Materials . European Synchrotron Radiation Facility. 2025. <https://doi.org/10.15151/ESRF-ES-658022426>.
 61. Dumazet A, De Mecquenem C, Theron, Chalmin E, Beauvoit E, Avranovich Clerici E, Albert-Tortosa F. Structural Analysis of Historical Materials . European Synchrotron Radiation Facility. 2025. <https://doi.org/10.15151/ESRF-ES-945457975>.
 62. Roisnel T, Rodriguez-Carvajal J. WinPLOTR: a Windows powder diffraction patterns analysis tool. *Mater Sci Forum.* 2001;378–381:118–23.
 63. Artesani A. Time-Resolved Photoluminescence in conservation science: study of crystal defects as markers of modern semiconductor pigments and of their degradation. Doctoral thesis, Politecnico di Milano. 2019.
 64. Coulier PJ. Question de la céruse et du blanc de zinc : envisagée sous les rapports de l'hygiène et des intérêts publics (The issue of lead white and zinc white: considered from hygiene and public interest perspective). Paris: J.-B. Baillière; 1852.
 65. Standage HC. The artists' manual of pigments: showing their composition, non-permanency, and adulterations, effects in combination with each other and with vehicles, and the most reliable tests of purity : together with the Science and Art Department's examination questions on painting. Crosby Lockwood and Co, London. 1887.
 66. Holley CD. The lead and zinc pigments. Hoboken: Wiley; 1909.
 67. Haddad A, Rogge CE, Martins A, Dijkema D. "Foundations of a great metaphysical style": unravelling Giorgio de Chirico's early palette. *Heritage Sci.* 2022;10(1):70.
 68. Bonaduce I, Duce C, Lluveras-Tenorio A, Lee J, Ormsby B, Burnstock A, van den Berg KJ. Conservation issues of modern oil paintings: a molecular model on paint curing. *Acc Chem Res.* 2019;52(12):3397–406.
 69. Zhang M, Averseng F, Krafft JM, Borghetti P, Costentin G, Stankic S. Controlled formation of native defects in ultrapure ZnO for the assignment of green emissions to oxygen vacancies. *J Phys Chem C.* 2020;124(23):12696–704.
 70. Artesani A, Gherardi F, Mosca S, Alberti R, Nevin A, Toniolo L, Valentini G, Comelli D. On the photoluminescence changes induced by ageing processes on zinc white paints. *Microchem J.* 2018;139:467–74.
 71. Eastaugh N, Walsh V, Chaplin T, Siddall R, editors. The pigment compendium: a dictionary of historical pigments. Oxford: Elsevier Butterworth-Heinemann; 2004.
 72. Macchia A, Cesaro SN, Keheyani Y, Ruffolo SA, La Russa MF. White zinc in linseed oil paintings: chemical, mechanical and aesthetic aspects. *Periodico di Mineralogia.* 2015;84(3):30–43.
 73. Vieille Montagne, editor. Blanc de zinc (Zinc white). Booklet edited by La Société de La Vieille Montagne. In French. After 1920.
 74. Hageraats S, Keune K, Stankic S, Stanescu S, Tromp M, Thoury M. X-ray nanospectroscopy reveals binary defect populations in sub-micrometric ZnO crystallites. *J Phys Chem C.* 2020;124(23):12596–605.
 75. Martins A, Albertson C, McGlinchey C, Dik J. Piet Mondrian's Broadway Boogie Woogie: non invasive analysis using macro X-ray fluorescence mapping (MA-XRF) and multivariate curve resolution-alternating least square (MCR-ALS). *Heritage Sci.* 2016;4:22.
 76. Govindaraju K, Roelandts I. Compilation report on trace elements in six anrt rock reference samples: diorite Dr-N, Serpentine Ub-N, Bauxite Bx-N, Disthene Dt-N, Granite Gs-N and Potash Feldspar Fk-N. *Geostand Newsl.* 1989;13(1):5–67.
 77. Palamara E, Das PP, Nicolopoulos S, Tormo Cifuentes L, Kouloumpis E, Terlixi A, Zacharias N. Towards building a Cathodoluminescence (CL) database for pigments: characterization of white pigments. *Heritage Sci.* 2021;9(1):100.
 78. Stoecklein W, Göbel R. Application of cathodoluminescence in paint analysis. *Scanning Microsc.* 1992;6(3):4.
 79. Kadikova I, Pisareva SA, Grigorieva IA, Lukashova M. Pigments of soviet Artists in the 1950s – Late 1970s. In: van den Berg KJ, Bonaduce I, Burnstock A, Ormsby B, Schaffr M, Carlyle L, Heydenreich G, Keune K, editors. Conservation of modern oil paintings. Cham: Springer; 2019. p. 165–89.
 80. Palladino N, Guillermot H, Marcos Alvarez E, Salvant J. Les peintures au blanc de zinc : du minerai à la palette (Zinc white paints: from the mineral to the palette). In French. Histoire de l'Art. Submitted in October 2023.

Publisher's Note

Springer Nature remains neutral with regard to jurisdictional claims in published maps and institutional affiliations.